

University of Nevada, Reno

Numerical and Experimental Analysis of the Effect of Faults in Open-Pit Mining Stability

A thesis submitted in partial fulfillment of the requirements for the degree of
Master of Science in Mining Engineering.

By

Babak Azarfar

Dr. Behrooz Abbasi, Thesis advisor

May 2019

Copyright by Babak Azarfar 2019

All Rights Reserved



THE GRADUATE SCHOOL

We recommend that the dissertation
prepared under our supervision by

BABAK AZARFAR

Entitled

**Numerical and Experimental Analysis of the Effect of Faults in Open-Pit
Mining Stability**

be accepted in partial fulfillment of the
requirements for the degree of

MASTER OF SCIENCE

Behrooz Abbasi, Ph.D. , Advisor

Javad Sattarvand, Ph.D. , Committee Member

Sean Warren, Ph.D. , Committee Member

Seyedsaeid Ahmadvand, Ph.D. , Committee Member

Robert (Bob) Watters Ph.D. , Graduate School Representative

David W. Zeh, Ph.D., Dean, Graduate School

May-2019

Abstract

This thesis addresses two main issues in slope stability: 1) effect of faults in the large open pit mines and large rock slopes, and 2) improving stability of tailing dams using Hydro-Jex[®] technology.

Section 1 - Effect of faults in the large open pit mines and large rock slopes: Deep open pit mines and large rock slopes expose many diverse rock lithologies and geological structures in a short period of time. Faulted rock masses reduce the integrity of slopes and can impose significant design challenges for geotechnical engineers. Numerical modeling is a powerful tool for simulating fault response. However, there are few guidelines and methods for calibrating/validating and implementing faults in a numerical model. This study presents a novel laboratory method to calibrate numerical models and highlights the challenges in simulating faults. The weak zone, ubiquitous-joint, and interface techniques are the widely-used methods in the modeling to capture fault slip mechanisms. One of the main issues in reliable modeling of faulted rock structure is the scarcity of experimental analyses in the laboratory under the controlled conditions.

Moreover, a comprehensive evaluation of the effect of using the conventional fault modeling methods on the stability of rock structures is required, as well as a benchmarking between theoretical and experimental results. This research combines theory and experiment, in order to fill the existing gaps, using numerical simulation and laboratory measurements. In the numerical simulations, sensitivity and comparative analyses are carried out to investigate the stability of rock slopes on large and small scales (overall open

pit slope and bench slope), and the fault zones, employing the methods as mentioned earlier in the *FLAC3D* software. The factor of safety of the slope is monitored upon variation of the design parameters, such as fault and rock mass mechanical properties, fault types, and modeling framework (e.g., mesh density, convergence ratio). Also, parameters such as shear displacement and shear stress are investigated to deduce the failure mechanism of the studied models. Finally, a laboratory test is performed to calibrate the modeling results and approximate the agreement between theoretical and experimental results. It needs to be mentioned that these analyses/tests are not to favor one method over the other, but rather to emphasize on pros and cons of each within the assumptions of this study.

Section 2 - improving stability of tailing dams using Hydro-Jex® technology:

Hydro-Jex® is a new enhanced method for heap leach treatments with significantly higher mineral recovery. In this study, the Hydro-Jex operation is case-studied at the Los Filos mine in Mexico for heap leach stability. This is pursued by numerical modeling of the heap leach pad stability and well monitoring of the phreatic surface before and after the Hydro-Jex operation. Experimental and numerical results both indicate an improvement in mineral processing under the influence of Hydro-Jex. Numerical results show an insignificant decrease and significant increase of stability during and after Hydro-Jex, respectively, while the integrity of the liner is maintained in both cases. The injection pressure is found to be negligible compared to the dimensionality of the heap and stability of the structure is not exposed to any significant risk, even up to 25% above the overburden pressure.

On the other hand, the heap leach factor of safety increases after Hydro-Jex attributed to the breakdown of the build-up water solution and thus a decrease in the

phreatic surface. The injection wells are suggested to be drilled in a wise manner based on accurate geophysical data; in locations where over-compaction of the heap material results in water solution build-ups and pore pressure enhancement. Compared to traditional heap leaching, the Hydro-Jex technique could not only expedite the mining process by increasing the chemical extraction, but also increase the stability of the heap by unclogging drains.

Dedication

I would like to dedicate my work to my lovely wife Shirin without her this journey never been started and to my parents who sacrificed their life for my future.

Acknowledgments

First and foremost, I express my sincere gratitude and indebtedness to my adviser Dr. Behrooz Abbasi, for allowing me to carry on the present topic and later on for his inspiring guidance, constructive criticism and valuable suggestions throughout these project works. I am very much thankful to him for his pain taking an effort in improving my understanding of these projects and his continued patience.

I am thankful to Prof. Robert Watters, Dr. Javad Sattarvand, Dr. Sean Warren and Dr. Seyedsaeid Ahmadvand for serving on my committee and providing me with very valuable comments. Moreover, special thanks to Dr. Seyedsaeid Ahmadvand for his support and contribution to publishing the results of this study.

I want to thank my brother, Arash Azarfar, for all of his support. I could never have started my study at the University of Nevada, Reno without his help.

I would also like to gratefully thank my kindest friend Dr. Mohammad Rezaee for all of his support, motivation and kind words in difficult times.

In the end, special thanks go to all faculty members of Department of Mining Engineering at the University of Nevada, Reno for their support.

Table of Contents

1. Chapter 1 – Introduction and Problem Statement	1
1.1. Background of the Study.....	1
1.2. Statement of the Problem	2
1.3. Goal and Specific Objectives	4
1.4. Overall Approach	5
1.5. Thesis Organization.....	6
2. Chapter 2 – Background and Model Development.....	7
2.1. Slope Stability	7
2.2. Factor of Safety	9
2.3. Fault Material Simulation.....	10
2.4. Theory And Background.....	11
2.4.1. Weak zone (WZ) method.....	11
2.4.2. Ubiquitous joint (UJ) method	12
2.4.3. Interface (IF) method	13
2.5. Laboratory Investigation	14
2.6. Heap Leaching Operation.....	14
2.7. Hydro-Jex® Technique	15

3. Chapter 3 – Effect of Fault in Rock Structure Stability (Numerical and Experimental Investigation)	17
3.1. Introduction	17
3.2. Methodology	19
3.2.1. Model Configuration.....	19
3.2.2. Mesh size evaluation.....	20
3.2.3. Material Properties.....	20
3.3. Sensitivity Analysis.....	21
3.3.1. Analysis 1 (Fault geometry).....	21
3.3.2. Analysis 2 (Convergence ratio – numerical stability).....	22
3.3.3. Analysis 3 (Mesh density)	23
3.3.4. Analysis 4 (Rock mass dilation)	23
3.3.5. Analysis 5 (Fault thickness).....	24
3.3.6. Analysis 6 (Fault Shear strength).....	24
3.4. Laboratory Tests Setup.....	24
3.5. Results and Discussion.....	27
3.5.1. Analysis 1 (Fault geometry).....	27
3.5.2. Analysis 2 (convergence ratio – numerical stability)	28
3.5.3. Analysis 3 (Mesh density)	31

3.5.4.	Analysis 4 (Rock mass dilation)	32
3.5.5.	Analysis 5 (fault thickness).....	33
3.5.6.	Analysis 6 (Fault shear strength)	35
3.5.7.	Failure mechanism	37
3.5.8.	Large Scale Results.....	38
3.5.9.	Laboratory Results	42
4.	Chapter 4 – Effect of Hydro-Jex Operation on the Stability of Heap Leach Pads: A Case Study of the Los Filos Mine, Mexico	45
4.1.	Introduction	45
4.2.	Model Development.....	46
4.3.	Results And Discussion.....	56
5.	Chapter 5 – Summary of the results and conclusion.....	64
5.1.	Summary of Results	64
5.1.1.	The Effect of Fault Zone on Rock Structure Stability	64
5.1.2.	The effect of Hydro-Jex technique on the stability of heap leach pad.....	67
5.2.	Future Work	67
	References.....	69

List of Tables

Table 3-1. Material properties used in numerical modeling	21
Table 3-2. Summary of the calculated FOS for planar sample.....	43
Table 3-3. Summary of the pull test results for the nonplanar sample	43
Table 4-1. Wells monitoring results prior to stimulation.....	48
Table 4-2. Pile properties for the numerical modeling	51
Table 4-3. Material properties for the numerical modeling	52
Table 5-1 Comprehensive comparison of three numerical methods for fault material simulation.....	65

List of Figures

Fig. 2-1. Shear strength reduction method (Azarfar et al. 2018)	9
Fig. 2-2 Fault material modeling methods: a) Weak zone (no preferred plane of weakness, isotropic material), b) Ubiquitous-Joint (non-isotropic material), c) Interface (discontinuous face).....	10
Fig. 2-3 Contours of dip angle along the fault plane captured by the UJ method.	11
Fig. 3-1 Schematic modeling of faulted structure and parameters that influence accuracy of the FOS value.	18
Fig. 3-2 Small-scale model geometry and boundary conditions.....	19
Fig. 3-3 Large-Scale model geometry and boundary conditions.....	20
Fig. 3-4 Different fault geometries: a) Nonplanar fault, b) Planar fault, c) Undulating nonplanar fault, d) Undulating planar fault.....	22
Fig. 3-5 Laboratory-scale model geometry and boundary conditions.	26
Fig. 3-6 3D scanning of the lab-scale nonplanar fault model.	26
Fig. 3-7 Laboratory pull test procedure and parameters.	27
Fig. 3-8 Fault roughness effect on the FOS for weak zone (WZ), interface (IF), and ubiquitous joint (UJ) methods.....	28
Fig. 3-9 Dependency of FOS on the convergence ratio, a) nonplanar fault, b) planar fault.	30

Fig. 3-10 Mesh density sensitivity analysis for the nonplanar fault.	32
Fig. 3-11 FOS versus dilation angle for the nonplanar fault.....	33
Fig. 3-12 FOS versus fault thickness for the nonplanar fault.	34
Fig. 3-13 Effect of the number of elements along the fault thickness.	35
Fig. 3-14 FOS versus cohesion for the nonplanar fault.	36
Fig. 3-15 FOS versus internal friction angle for the nonplanar fault.....	36
Fig. 3-16 Failure mechanism.	38
Fig. 3-17 Displacement contours, using WZ method.	40
Fig. 3-18 Displacement contours, using UJ method.....	40
Fig. 3-19 Failure mechanism obtained by WZ method..	41
Fig. 3-20 Failure mechanism obtained by UJ method.	41
Fig. 4-1. Drawing of zones impacted by the pumping of the solution down a perforated Hydro-Jex [®] well.....	46
Fig. 4-2. Electrical resistivity survey across a leach pad at the Los Filos Mine used to build the phreatic surface and pore pressure in numerical modeling.	48
Fig. 4-3. The model geometry and location of Hydro-Jex wells.	49
Fig. 4-4. Pore pressure counters in the model and across the electrical resistivity survey lines.....	50

Fig. 4-5. The schematic representation of cavity initiation and washout of fines near the wellbore.....	53
Fig. 4-6. The schematic treatment (a to n) and drain down from each zone in a Hydro-Jex® well pumping stimulation	54
Fig. 4-7. Displacement before the Hydro-Jex operation at the heap leach pad.	57
Fig. 4-8. Displacement of the heap leach pad after the Hydro-Jex operation.....	58
Fig. 4-9. The effect of phreatic surface depth on the FOS value.	59
Fig. 4-10 The effect of phreatic surface depth on the displacement in the heap leach pad..	59
Fig. 4-11. Pore pressure counters before and during the Hydro-Jex operation..	61
Fig. 4-12. Displacement of the heap leach pad during the Hydro-Jex operation wellbore HJ.6.	61
Fig. 4-13. The effect of injection zone pressure on FOS.	62
Fig. 4-14. The effect of injection zone pressure on the displacement around the well. ...	63

1. Chapter 1 – Introduction and Problem Statement

The material of this thesis has been collected from three papers:

- “A Discussion on Numerical Modeling of Fault for Large Open Pit Mines” has been presented and published in the 52nd U.S. Rock Mechanics/Geomechanics Symposium.
- “Stability Analysis of Rock Structure in Open-Pit Mine: Numerical and Experimental Fault Modeling” in Rock Mechanics and Rock Engineering journal (RMRE).
- “The Effect of Hydro-Jex Operation on the Stability of Heap Leach Pads: A Case Study of the Los Filos Mine, Mexico” in Mining, Metallurgy & Exploration” journal.

1.1. Background of the Study

Slope stability analysis is a critical component parts of the design stage in mining and civil engineering projects. One of the outcomes of slope stability analysis in open-pit mining is factor of safety (FOS), overall slope of mine and bench slope. For optimum slope design, technical parameters (such as rock mass properties, presence of geological features, etc.), economical parameters (such as mine life, optimum pit design, commodity price, etc.), government regulations and policies (e.g., minimum factor of safety) and possible safety issues during mining activity should be considered. The accuracy of FOS is critical. Overestimation of FOS may increase the possibility of slope failure and the risk to mining activity.

On the other hand, underestimation of FOS may increase the safety level in mining activity but reduces the mineable reserve and mining profitability. Nowadays, with the growth of global demand for minerals on one side, and technology advancements on the other side, the depth of open-pit mines has significantly increased, and mining companies are now considering deeper and steeper designs. With depth increase of an open-pit mine, the chance of presence of complex rock lithologies and geological structures (e.g., faults and bedding planes) will increase which may impact the rock slope stability.

Numerical modeling methods are used to investigate and design several underground and open-pit mining operations within the industry. Numerical modeling is a powerful tool for simulating slope stability of large and deep open-pit mines and analyzing the impact of several factors such as complex rock lithologies, geological structures and water condition on slope stability. Using numerical modeling improves the understanding of slope behavior and deformation processes in 2D and 3D dimensions. Also, it is possible to address areas or situations where the stability of the slope may be compromised. Numerical modeling can be used as a predictive tool, a mechanism for parametric study, or as an investigation tool for better understanding the effect of new technology, the behavior of the material in different conditions and mechanisms of failure. Because of the dependency of final results on the input data and simulation method, they should be validated with the experimental or analytical methods.

1.2. Statement of the Problem

Mining accidents in recent decade, such as Betze-Post (Rose & Hungr, 2007), Bingham Canyon (Septian, et al., 2017) in the USA and Batu Hijau in Indonesia (Kristiono, et al., 2015), show the possibility of large slope failure due to the increase of mining depth and

as a result, presence of complex rock lithologies and geological structures. Available statistics show that almost all failures in open-pit mining are structural control failures (Patton, 1966; Hopkins, et al., 1975; Hoek & Bray, 1981; Wiles, 2014; Tutluoglu, et al., 2015; Sun, et al., 2016). The mining accidents demonstrate the importance of doing a comprehensive study on the impact of geological discontinuities on slope stability. Although, several studies have been conducted using numerical methods for slope stability analysis (Hammah, 2004; Cala, et al., 2006; Zhang, et al., 2011; Wiles, 2014; Chen, et al., 2015; Tutluoglu, et al., 2015; Sun, et al., 2016; Fu, et al., 2017; Tang, et al., 2017; Park & Michalowski, 2017). But, due to the difficulty of characterizing the fault slip mechanisms, there are few guidelines for simulating faults in numerical models (Mostyn, et al., 1997; Zheng, et al., 2014; Alzo'ubi, 2016; Tang, et al., 2017). Therefore, lack of a comprehensive study on all available methods for fault simulation is apparent.

Nowadays, slope back analysis and displacement monitoring are the only methods available to calibrate the slope numerical models and evaluate fault shear strength. These techniques rely on a mobilized or failed slope (assuming FOS=1.0) to calibrate the accuracy of the computational model. In the absence of such a condition (failed slope or accurate displacement measurements), to the best of the authors' knowledge, there is no available laboratory technique evaluating the capability of fault models in rock structures.

To respond to the increasing global demand for minerals and reduce the cost of the mining operation, researcher and scholars try to propose new methods to improve the efficiency of existing procedures. Any recently proposed method may introduce some technical, environmental and financial concerns at different levels. The Hydro-Jex[®] technique, introduced by Seal (Seal, 2007; Seal, 2004), improves the recovery and reduces

the extraction time in the leaching process. Hydro-Jex has shown to recover the stranded metal inventory from the pad at a faster leaching rate due to the increase of in-situ pressure, resulting in particle fluidization, improved micropore wetting, and reagent effectiveness, while reducing the time of rinsing, pumping, and closure (Seal, 2007; Seal & Jung, 2005). Also, it can optimize the chemical composition of targeted zones and operational costs compared to conventional techniques (Seal, et al., 2012). Although this method has been used in a few mines with no reported issues, because of the catastrophic impact of a heap leach pad failure (e.g. Summitville (Plumlee, et al., 1995), Cieneguita (Anon., 2018), and Pará mines (Anon., 2018), a comprehensive study of the effect of Hydro-Jex operation on the stability of heap leaching pad is necessary.

1.3. Goal and Specific Objectives

The main objective of this study is to capture the impact of the fault material simulation method on the overall stability of large and deep open-pit mines. The study is helpful for a better understanding of the failure mechanism in a complex situation. This research proposes a novel laboratory method for the validation of numerical results and answers stability concerns regarding using the Hydro-Jex technique.

The specific goals of this study are summarized as follow:

- Considering all available methods for fault material simulation in FLAC3D software and conducting a comparative study to point out advantages, disadvantages, and applications of each method.
- Carrying out a parametric study on the sensitivity of each method regarding the modeling parameters, rock mass, and fault material properties and fault geometry,

and finding the optimum threshold for each parameter to reduce the computational cost and time and increase the accuracy of the final results.

- Conducting a comprehensive study on the effect of fault material simulation on the failure mechanism.
- Developing a novel laboratory method to calculate the slope Factor of safety (FOS) and simulate the mechanics of failure in a controlled manner for validating numerical modeling results.
- conducting a comprehensive study on the effect Hydro-Jex technique on the overall stability of heap leach pad and addressing concerns using FLAC3D.

1.4. Overall Approach

The overall approach of this study is summarized as follows:

- Using FLAC3D software for numerical simulation,
- Conducting sensitivity analysis to capture the optimum threshold for input data on the small-scale modeling (one bench of open-pit mine),
- Removing the scale effect on the results by simulating the whole open pit mine (large- scale simulation),
- Designing and developing the experimental test (laboratory scale) to validate the numerical results,
- Using field data to validate/calibrate the numerical models.

1.5. Thesis Organization

This thesis is presented through 5 chapters. The chapter organization of this thesis is based on the three papers above. The chapter titles are as follows:

- Chapter 1– Introduction and Problem Statement
- Chapter 2 – Background and Model Development
- Chapter 3 – Effect of Fault in Rock Structure Stability (Numerical and Experimental Investigation)
- Chapter 4 –Effect of Hydro-Jex Operation on the Stability of Heap Leach Pads:
A Case Study of the Los Filos Mine, Mexico
- Chapter 5 – Summary of the Results and Conclusion

2. Chapter 2 – Background and Model Development

2.1. Slope Stability

Determining slope stability is a critical part of the design stage of mining and civil engineering. In an open-pit mine, a slope failure may result in delayed production, fatality, and equipment loss (Duncan, 1996; Stacey, Xianbin, Armstrong, & Keyter, 2003). With the growth of modern technologies and global demand for minerals, the depth of open-pit mines has increased significantly. This has imposed several design challenges in slope engineering and potentially increased the risk of large slope failures (Franz, 2009; Sjöberg, Hustrulid, McCarter, & Van Zyl, 2000; Stacey et al., 2003; Tutluoglu, Ferid Öge, & Karpuz, 2011).

In deep open pit mines, more complex rock lithologies are exposed, and they can interact with geological structures (e.g., faults, bedding planes) and impact the rock slope stability. The structural characteristics of the slope, such as geometry, geological features, and rock mass properties are some of the key factors affecting slope stability (Stead & Wolter, 2015). For instance, geological discontinuities such as faults, and their properties (shear strength properties, dip (D), and dip-direction (D-D)) determine the failure mechanism (Raghuvanshi, 2019).

Several techniques are used in determining slope stability. Calculating the factor of safety (FOS), which is defined as the ratio of actual shear strength to the minimum shear stress required to maintain equilibrium (Eq. (2.1)), is a common approach to evaluate the slope stability in numerical modeling (Bishop 1955; Matsui and San 1992; Fleurisson 2012; Taleb Hosni and Berga 2016). In this definition, the FOS value of unity represents

imminent failure.

$$\text{FOS} = \frac{\text{Shear Strength of Rock mass or Soil}}{\text{Shear Stress required to prevent failure}} \quad (2.1)$$

Stress ratio, defined as the ratio of the maximum unbalanced force (MUF) to the representative internal force, is another equilibrium criterion typically determined for slope stability (Sharma & Kaur, 2016). Also, the ratio of the MUF to the total applied force, known as the solve ratio, is useful in slope stability evaluations (Itasca, 2017). As one of the commonly-used techniques, the shear strength reduction (SSR) method reduces the shear strength properties of the rock mass until a failure happens (Dawson, Roth, & Drescher, 1999; Duncan, 1996; Gupta et al., 2016; Hammah, Yacoub, Corkum, Wibowo, & Curran, 2007; Yang, Zhu, & Zou, 2012; You, Mandalawi, Soliman, Dowling, & Dahlhaus, 2018; Zienkiewicz, Humpheson, & Lewis, 1975).

Dilation is another important factor in the failure analysis of soil rock and granular materials; dilation is defined as the volume change upon shear deformation (Vermeer, 1998). Dilation becomes essential in the after-failure and plasticity analyses of the rock material. It has been demonstrated that dilation is interconnected with the cohesion and internal friction angle of the material (Alejano & Alonso, 2005). Since the fault zone consists of weak material, such as breccia and soil, dilation is expected to affect the FOS of the slope. However, current methods consider dilation only after failure, and in this sense, they may overestimate the slope stability.

2.2. Factor of Safety

The SSR method reduces the input cohesion, tensile strength (T_s), and internal friction angle of the material by the same factor (Eq. (2.2), Fig.2.1), and the final strength reduction factor (SRF) represents the FOS (Dawson et al., 1999).

$$FOS = SRF = \frac{C_0}{C_r} = \frac{\tan \varphi_0}{\tan \varphi_r} \quad (2.2)$$

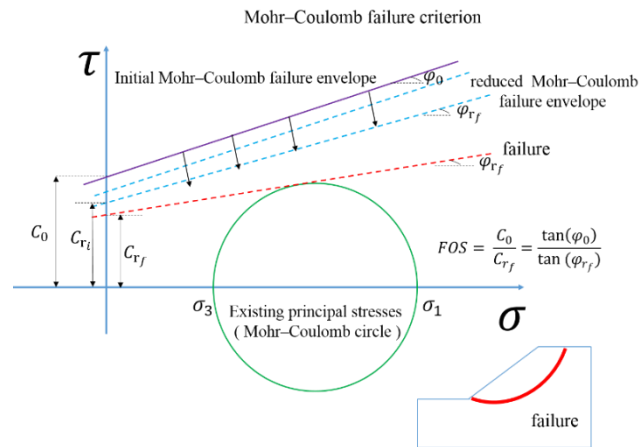


Fig. 2-1 Shear strength reduction method (Azarfar et al. 2018)

Iteratively, the SSR method reduces the strength properties (C_0 , T_s and φ_0) by an incremental SRF until a failure happens and repeats this procedure until reaching the smallest intervals within the range of acceptable error. The FOS value for a large open pit mine usually is reported to no more than two decimals.

2.3. Fault Material Simulation

Numerical modeling is often used for simulating complex slope stability and fault effects, However, there are not many analytical methods (Cala et al. 2006; Hammah et al. 2007; Tutluoglu et al. 2011; Zhang et al. 2011; Wiles 2014, Sun et al. 2016; Tang et al. 2017; Park and Michalowski 2017). Also, there are few guidelines for fault simulation in numerical modeling due to difficulties in characterizing the fault slip mechanism (Alzo'ubi, 2016; Mostyn, Helgstedt, & Douglas, 1997; Tang et al., 2017; Zheng, Chen, Zhu, Liu, & Cheng, 2013). Three widely-used numerical methods for fault modeling are weak zone (WZ), ubiquitous joint (UJ), and interface (IF), each of which introduces the fault in different way. In the WZ method, the fault material is treated as a weak zone (fault material properties, Fig. 2-2,a) with no preferred weakness direction. The UJ method models the fault as a zone with a preferred weakness direction oriented in the direction of the fault plane (ubiquitous-joint, Fig. 2-2,b). In this method, the dip and dip direction of the fault surface can be accurately implemented in the model (Fig. 2-3). In the IF method, the fault has zero thickness and fault elements contact at an interface (discontinuous face) which defines the fault direction (Fig. 2-2,c).

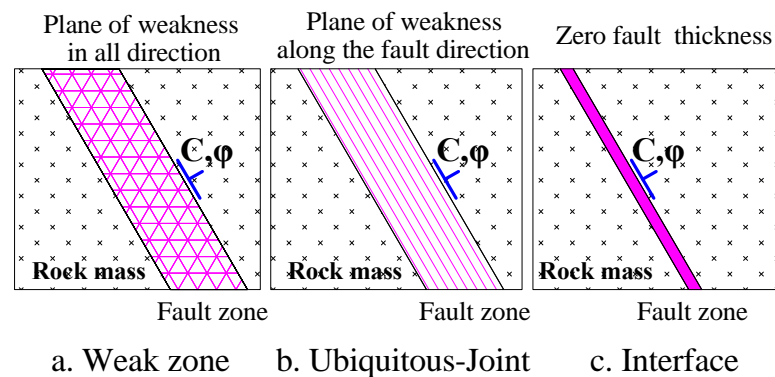


Fig. 2-2 Fault material modeling methods: a) Weak zone (no preferred plane of weakness, isotropic material), b) Ubiquitous-Joint (non-isotropic material), c) Interface (discontinuous face).

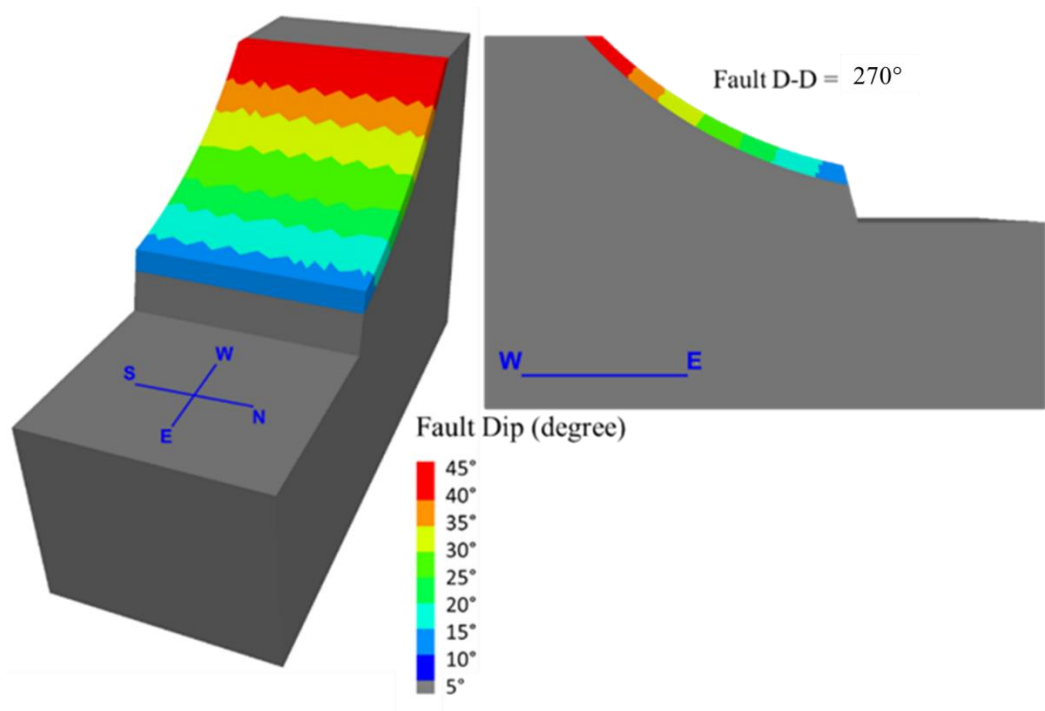


Fig. 2-3 Contours of dip angle along the fault plane captured by the UJ method.

2.4.Theory And Background

2.4.1. Weak zone (WZ) method

In the WZ method (Fig. 2-2,a), the fault material and properties are treated as an isotropic medium (with no preference plane of weakness). In other words, the fault mechanical properties were assigned to the zone without defining the dip and dip direction of the fault plane. In this study, the WZ failure envelope follows the Mohr-Coulomb criterion (shear yield function) with a tension cutoff (tension yield function). On this

envelope, the non-associated and associated flow rules control the position of a stress point for shear and tension failures, respectively (Itasca, 2017).

2.4.2. Ubiquitous joint (UJ) method

The UJ method introduces a specific dip and dip-direction as a virtual weak plane for the fault material (Fig. 2-2,b). It is important to realize that this method does not introduce a single plane of weakness, whereas the zone/material has weaker properties in a specific direction (anisotropic behavior). The failure criterion for the plane consists of a composite Mohr-Coulomb envelope with a tension cutoff. The non-associated and associated flow rules control the position of a stress point for shear and tension failures, respectively (Itasca, 2017; JIANG, 2009). In the UJ method, the relevant plastic corrections are made after general failure is detected. Slip will occur on the discontinuity if the following condition is satisfied (Sainsbury & Sainsbury, 2017):

$$1 - \tan\varphi_j \tan\beta > 0 \quad (2.7)$$

$$\sigma_1 \geq \sigma_3 + \frac{2(c_j + \sigma_3 \tan\varphi_j)}{(1 - \tan\varphi_j \tan\beta) \sin 2\beta} \quad (2.8)$$

Based on Eq. (2.7) and (2.8), if $1 - \tan\varphi_j \tan\beta < 0$, slip occurs in the rock mass rather than discontinuity. In other words, failure cannot happen along the discontinuities if $\beta < \varphi$ or $\beta=90$. Also, the normal and shear stress on the joint can be calculated from,

$$\sigma_n = \frac{1}{2}(\sigma_1 + \sigma_3) + \frac{1}{2}(\sigma_1 - \sigma_3) \cos 2\beta \quad (2.9)$$

$$\tau = c_j + \sigma_n \tan\varphi_j \quad (2.10)$$

$$\tau = \frac{1}{2}(\sigma_1 - \sigma_3)\sin 2\beta \quad (2.11)$$

$$\sigma_1 - \sigma_3 = \frac{2(c_j + \sigma_3 \tan \varphi_j)}{(1 - \cos \beta \tan \varphi_j) \sin 2\beta} \quad (2.12)$$

2.4.3. Interface (IF) method

In the IF method, the fault material is introduced into the model as planes on which sliding or separation can occur (Fig. 2-3, c). The characteristics of this interface are defined by normal and shear stiffness as well as sliding properties (Itasca, 2017). Friction, cohesion, dilation, and tensile and shear bond strength are the properties used in the IF method. The normal and shear stiffness (k_n and k_s) parameters control the elastic deformation normal and along the face of the interface elements. In this study, these parameters were assumed constant. Interface elements introduce a mechanical contact between two zone surfaces, each of which is defined by three nodes (triangular element). The interface elements allow in continuous numerical modeling, two adjacent zones to be separated and to behave individually. Eq. (2.3) and (2.4) show the normal and shear forces at each time step ($t + \Delta t$),

$$F_n^{(t+\Delta t)} = k_n u_n A + \sigma_n A \quad (2.3)$$

$$F_{si}^{(t+\Delta t)} = F_{si}^{(t)} + k_s \Delta u_{si}^{(t+0.5\Delta t)} A + \sigma_{si} A \quad (2.4)$$

In addition, the maximum shear force is limited by the Coulomb shear-strength criterion and can be calculated by Eq. (2.5). If the actual shear force is more than the allowable shear force, sliding occurs. The effective normal stress on the discontinuities varies with respect to shear displacement during sliding (Eq.2.6).

$$F_{smax} = cA + \tan\varphi (F_n - pA) \quad (2.5)$$

$$\sigma_{ni} = \sigma_n \frac{|F_s|_o - F_{smax}}{Ak_s} \tan\psi k_n \quad (2.6)$$

2.5.Laboratory Investigation

Currently, slope back analysis is the only method to calibrate the slope numerical models and evaluate fault shear strength. This technique relies on a mobilized or failed slope (assuming FOS=1.0) to calibrate the accuracy of the computational model. In the lack of such a condition (failed slope or accurate displacement measurements), to the best of the authors' knowledge, there is no available laboratory technique evaluating the capability of fault models in rock structures. In this study, a novel laboratory method was proposed to calculate slope FOS and simulate mechanics of failure in a controlled manner. This experiment was used to calibrate and quantify the error magnitude associated with different numerical modeling approaches. Considering the possible sources of error, choosing an appropriate numerical method in modeling a fault is crucial to avoid under/overestimation of the stability. As much as over-estimation (reporting higher FOS value) risks the stability of the system, lower-estimation (reporting lower FOS value) may reduce the mineable reserve and profit.

2.6.Heap Leaching Operation

The heap leaching operation is a well-developed and widely-used operation in the mining industry to process low-grade materials and minimize environmental impacts (Petersen, 2016; Mandziak & Pattinson, 2015). On the other hand, a catastrophic heap leach pad failure has significant financial and environmental consequences, e.g., Summitville

(Plumlee, et al., 1995), Cieneguita (Anon., 2018), and Pará mines (Anon., 2018). One of the important stages of leach pad design is the stability analysis concerning the leaching method. Sliding of material along the slope, tensile tearing of the geomembrane, and failure of the geomembrane anchorage are three main instability factors (Mortazavi, et al., 2015; Karimi Nasab, et al., 2001). The critical surface failure depends on the shear strength of the weakest material in the heap, such as the ore, protection layer, and liner (Zanbak, 2012). The factor of safety (FOS) is often used to evaluate the stability of leach pads (Coulibaly, et al., 2017; Reyes, et al., 2016; Reyes, et al., 2014). The FOS values of 1.5 and 1.3 are the lowest safety limits of the heap structure with and without an internal pond, respectively. (Zanbak, 2012), where FOS=1.0 is universally accepted as the imminent failure.

2.7. Hydro-Jex® Technique

The heap leaching operation usually covers many hectares of land, tonnes of low-grade ore, low recovery percentage, and long extraction time (Ghorbani, et al., 2016). Many alternative methods have been developed to overcome challenges in this operation (Winterton & Rucker, 2013; Padilla, et al., 2008), one being the Hydro-Jex® technique, introduced by Seal (Seal, 2007; Seal, 2004). Hydro-Jex has shown to recover the stranded metal inventory from the pad at a faster leaching rate due to the increase of in-situ pressure that creates slope stability concern, resulting in particle fluidization, improved micropore wetting, and reagent effectiveness, while reducing the time of rinsing, pumping, and closure (Seal, 2007; Seal & Jung, 2005). Also, it can optimize the chemical composition of targeted zones and operational costs compared to conventional techniques (Seal, et al., 2012). In the Hydro-Jex operation, a significant amount of fluid is injected into the discrete areas within the heap, affecting its regional pore pressure and thus structural stability

(Ulrich, 2008). The phreatic surface, injection pressure, and liner integrity are the main stability concerns of applying Hydro-Jex in the heap leaching (Ulrich, 2008). The liner integrity becomes critical during both well drilling and high-pressure injection. In the lower limit of effective stress and shear strength, sliding off the heap occurs due to excessive injection of the chemical fluid (Ulrich, 2008). The Hydro-Jex operation efficiently works on the pressures close to the total vertical stress. If the high-pressure Hydro-Jex fluids propagate radially outward from the casing, a weak sliding plane can be possibly formed. A 15 m saturated zone around the casing is reported as the distance at which the maximum hydraulic rechanneling of material occurs for overcoming overburden pressure (Rucker, 2015; Rucker, et al., 2009).

3. Chapter 3 – Effect of Fault in Rock Structure Stability (Numerical and Experimental Investigation)¹

3.1. Introduction

The overall approach of slope stability analysis and fault materials simulation is shown in Fig. 3-1. The slope stability analysis has a different response concerning the geometry, shear band, fault material properties and method used to model the faulted zone (WZ, UJ or IF). Model calibration/validation is an essential step in any numerical modeling to obtain representation within the acceptable margin of uncertainties.

¹ This chapter has been submitted in the scientific journal “Rock Mechanics and Rock Engineering” with the title of “Stability Analysis of Rock Structure in Open-Pit Mine: Numerical and Experimental Fault Modeling”. also the result of sensitivity analysis for small scale simulation (one bench of open-pit mine) has been published in” 52nd US Rock Mechanics / Geomechanics Symposium, 2018” with title of “A Discussion on Numerical Modeling of Fault for Large Open Pit Mines” and accessible at <https://www.onepetro.org/conference-paper/ARMA-2018-080>

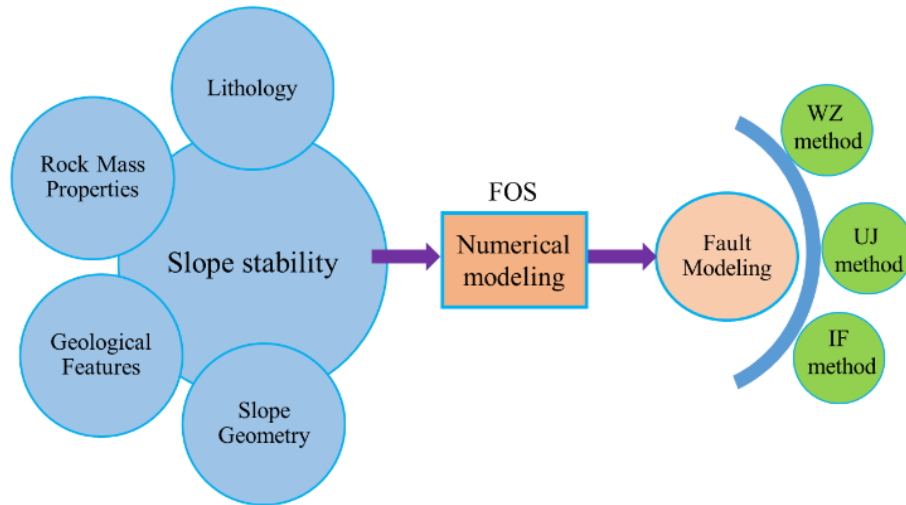


Fig. 3-1 Schematic modeling of faulted structure and parameters that influence the accuracy of the FOS value.

In this thesis, the WZ, UJ, and IF methods were used to simulate the fault behavior, and the SSR method was used to calculate the FOS values. To reduce the run time, a sensitivity analysis was carried out in the small-scale and eventually extended to large-scale modeling. For the small-scale, one typical bench of an open-pit mine was simulated, and for the large-scale, the whole open-pit mine was modeled. Laboratory-scale and empirical equations were used to provide a benchmark for modeling results. All simulations were performed in the *FLAC3D* software, in which a finite difference method (FDM) was used.

3.2. Methodology

3.2.1. Model Configuration

To model the open-pit bench(es), homogeneous isotropic modeling was used. All models were constrained at the bottom (x , y , z -direction) and in the normal direction (perpendicular to the side plane) on the sides (N-S and E-W faces). The geometry of the bench was modeled in the Rhino 3D software and then imported to the *FLAC3D* (Fig. 3-2). The same approach was used for the large-scale model, with the overall pit slope of 44° and bench height of 10 meters (Fig. 3-3).

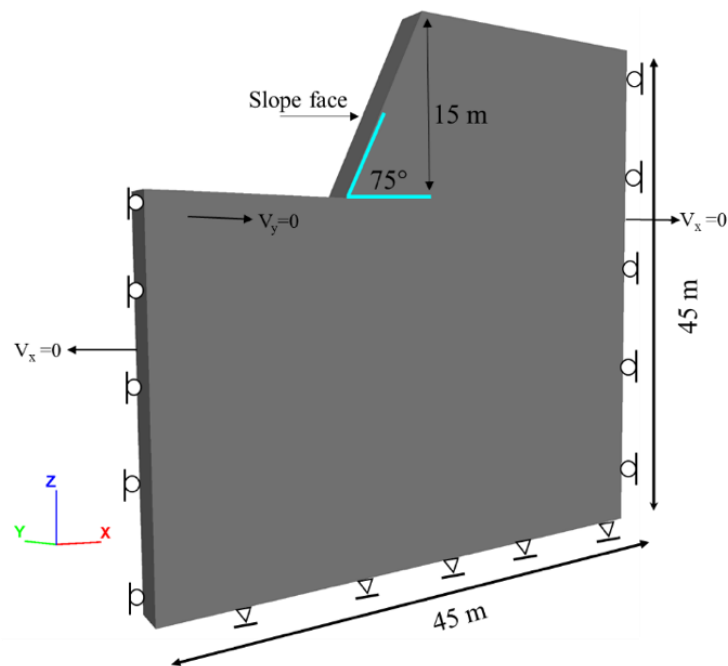


Fig. 3-2 Small-scale model geometry and boundary conditions.

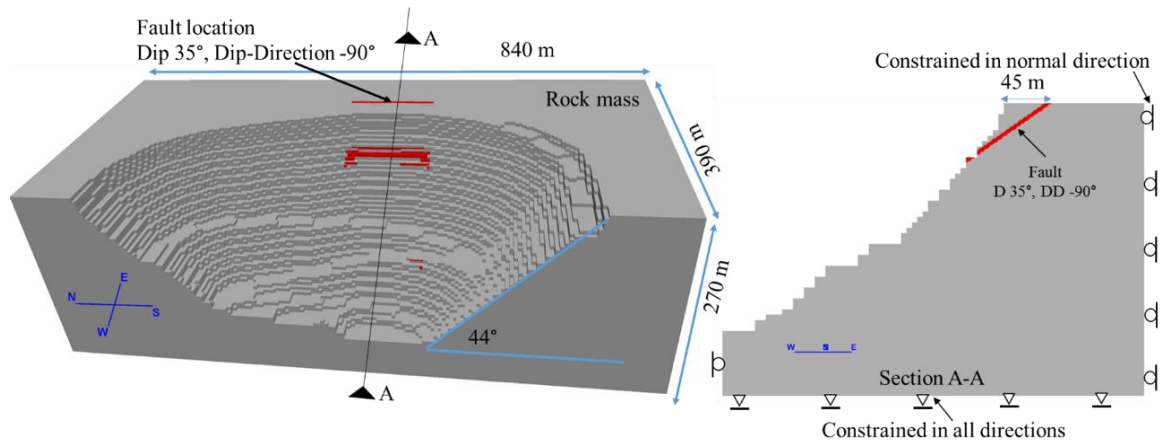


Fig. 3-3 Large-Scale model geometry and boundary conditions.

3.2.2. Mesh size evaluation

For the small- and large-scale modeling, brick elements were used as the dominant mesh geometry, and around the fault plane due to the complexity of the fault shape tetrahedral elements were used (hybrid meshing). The nodal mixed discretization (NMD) technique (Abbasi, Russell, & Taghavi, 2013) was implemented to capture more volumetric flexibility and improve the plasticity of the structure. For all models, the number of tetrahedra per volume of interest (NTV) was set to 60 to create a balance between accuracy and modeling cost (Abbasi et al., 2013).

3.2.3. Material Properties

The rock mass was modeled as an elastic-plastic material using the Mohr-Coulomb failure criterion. Typical properties of a competent rock mass were used in the modeling to ensure the failure happens through the faulted zone (Table 3-1). The fault material properties were set similar to those of clayey soil.

Table 3-1. Material properties used in numerical modeling

Material Properties	Rock Mass	Fault	Units
Density	2500	2100	kg.m ⁻³
Bulk modulus	3×10 ⁹	4.7×10 ⁷	Pa
Shear modulus	1.5×10 ⁹	3.3×10 ⁷	Pa
Cohesion	1×10 ⁶	25×10 ⁴	Pa
Internal friction angle	36	20	degree
Tension strength	1×10 ⁵	0	Pa
Normal-stiffness	N/A	1×10 ⁸	Pa.m ⁻¹
Shear-stiffness	N/A	1×10 ⁸	Pa.m ⁻¹

3.3. Sensitivity Analysis

The sensitivity analysis was performed by monitoring the stability behavior concerning changes of different variables in the small-scale faulted structure (single bench) modeled by WZ, IF, and UJ methods. In some sensitivity analyses, parameters such as mesh density and solve ratio are used to find the thresholds above which the stability is independent of parametric changes. After that, these thresholds were applied for other sensitivity analysis.

3.3.1. Analysis 1 (Fault geometry)

The effect of fault geometry on the slope stability was analyzed for different geometries: planar, nonplanar, undulated planar, and undulated nonplanar faults (Fig. 3-4).

A fault trace usually is not straight and usually contains undulations; this may cause interlocking and rock bridges. These features change the fault shear strength and failure mechanics. The goal of this sensitivity study is to evaluate the performance of each numerical method (WZ, UJ, and IF) in simulating fault interlocking behavior.

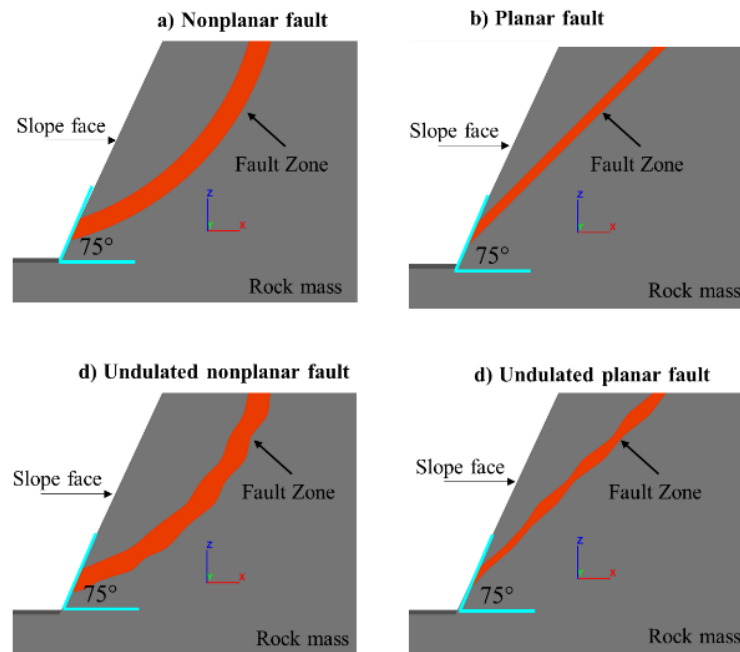


Fig. 3-4 Different fault geometries: a) Nonplanar fault, b) Planar fault, c) Undulating nonplanar fault, d) Undulating planar fault.

3.3.2. Analysis 2 (Convergence ratio – numerical stability)

FLAC3D uses an implicit numerical technique for obtaining numerical approximations to the solutions of time-dependent partial differential equations (PDE). Strong convergence criteria are necessary for any numerical scheme for the stability of PDE in the initial value problems. Assuming that the PDE is stable, the convergence rate and step size are critical to reach a robust numerical solution (near exact solution). For simplicity in FLAC3D, the convergence ratio is called solve ratio. In this study, the

sensitivity of FOS value with a variation of the solve ratio was studied. The solve ratio was allowed to incrementally decrease from 10^{-5} to 10^{-8} to highlight its impact on the FOS value. More details on threshold criteria are discussed in Azarfar et al. 2018. It should be mentioned that in some cases a number of numerical iterations can also be important in estimating the FOS value.

3.3.3. Analysis 3 (Mesh density)

In this sensitivity analysis, the FOS of a non-planar fault was obtained for different mesh densities. It has been shown that higher mesh density in numerical modeling results in higher accuracy, especially in finite element methods (Ghavidel, Mousavi, & Rashki, 2018). However, this analysis was performed to approximate a threshold after which the FOS value improvements would not justify the computational burden. Moreover, reaching the mesh density threshold of small scale is not affordable in large scale modeling and approximating the resultant errors is essential.

3.3.4. Analysis 4 (Rock mass dilation)

This analysis was carried out to investigate the stability sensitivity to the dilatational behavior of the fault zone. This was captured by changing the dilation angle of the fault material using either the corresponding associated or non-associated flow rules. The associated flow rule was used when the dilation angle was equal to the internal friction angle, and the non-associated flow rule was used otherwise.

3.3.5. Analysis 5 (Fault thickness)

Fault zone thickness is an important parameter for many geotechnical designs. A typical fault thickness can be varied from 1 mm to 10 meters, and it controls the fault shear displacement. In the fault thickness analysis, the FOS was calculated for different thicknesses of the non-planar fault. This was performed for the WZ and UJ methods, as the IF, by definition, is in contact with and lacks a separation between the elements of the fault zone. Often, the real thickness of the fault zone cannot be implemented in large scale modeling due to the mesh density limitation and computational cost.

3.3.6. Analysis 6 (Fault Shear strength)

Obtaining an intact sample of fault gouge or filling material is very difficult and requires high experience. Using limited and disturbed field samples (or remolded samples) decreases the accuracy of laboratory tests and design inputs. Sensitivity on shear strength of the fault material will be a guideline to consider the error associated with the lack of laboratory results. Cohesion and internal friction angle parameters were used to analyze the sensitivity of each method to the shear strength properties (tension strength = 0) of the fault material. The FOS value was calculated for different inputs of the aforementioned properties. These parameters will be changed through the SSR process. However, there is always uncertainty in the determination of initial values.

3.4. Laboratory Tests Setup

Two bench samples were built in the laboratory (non-cohesive planar and nonplanar faults) using concrete to evaluate the fault modeling techniques (IF, WZ and UJ) (Fig. 3-5). For non-cohesive material, friction angle is the most important factor governing the failure

mechanism. The friction angle of the planar model was measured according to the US Bureau of Reclamation (USBR 6258-09) standards, using a manual tilt desk and a digital clinometer. This measurement was repeated (90 measurements, standard deviation (SD)= 0.549) to ensure a reasonable precision among results. The median value of the friction angle and the measured dip angle were used to calculate the FOS based on the analytical formulation (Eq. (3.1)). To make a comparison between simulation and experiment, two samples with the same properties were modeled in FLAC3D software, based on laboratory-made models (Fig. 3-5). To adjust the size and geometrical compatibility between the simulation and laboratory models, the latter was 3D scanned (Artec Spider 3D scanner, accuracy = 0.05 mm, resolution = 0.1 mm) and then transferred to the modeling software. Fig. 3-6 shows the test procedure of 3D scanning for the nonplanar sample. A pull test was performed to obtain the force required for failure in the laboratory (Fig. 3-7). This force was also calculated from Eq. (3.2) and compared with the pull force of the planar model to find the correction factor. The correction factor was used to calibrate the failure pull force of the nonplanar model, for which the formula (Eq. 14) is not applicable directly.

$$FOS = \frac{cA + W\cos\beta\tan\varphi}{W\sin\beta} \xrightarrow{c=0} FOS = \frac{\tan\varphi}{\tan\beta} \quad (3.1)$$

$$FOS = \frac{(W\cos\beta - F\sin\beta)\tan\varphi}{W\sin\beta + F\cos\beta} \quad (3.2)$$

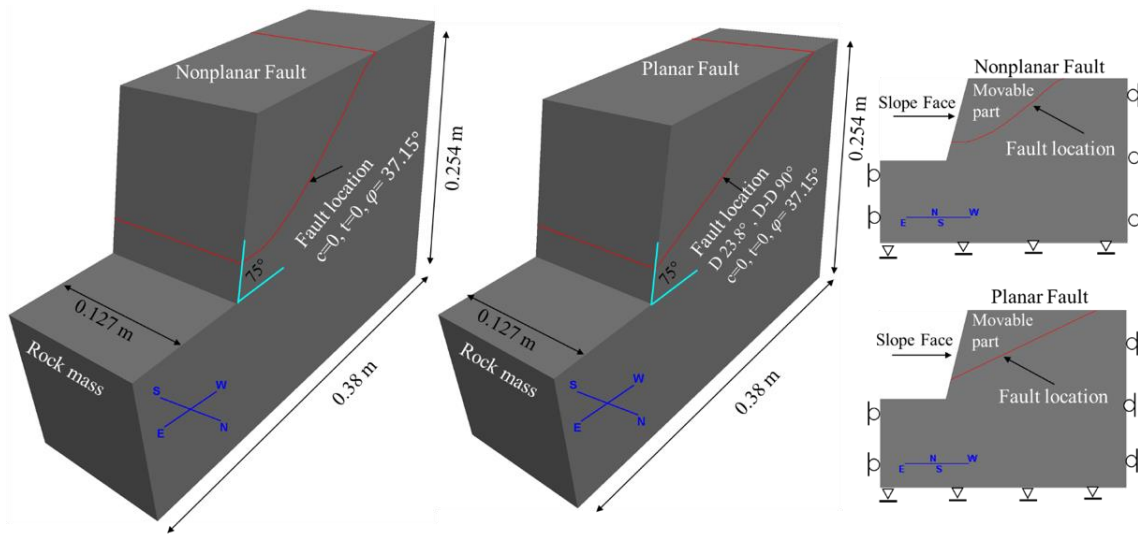


Fig. 3-5 Laboratory-scale model geometry and boundary conditions.

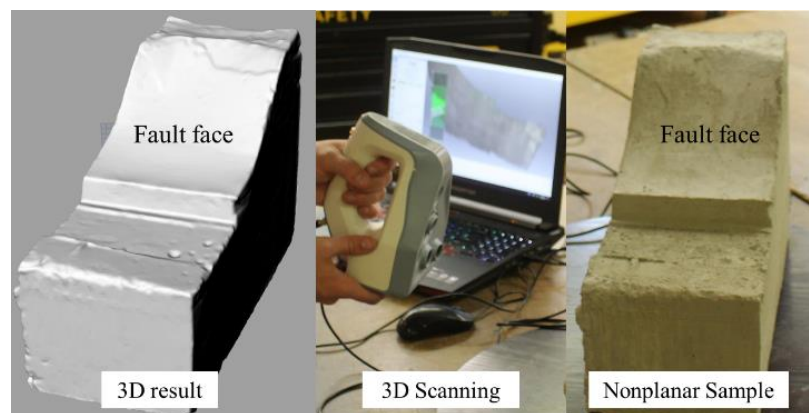


Fig. 3-6 3D scanning of the lab-scale nonplanar fault model.

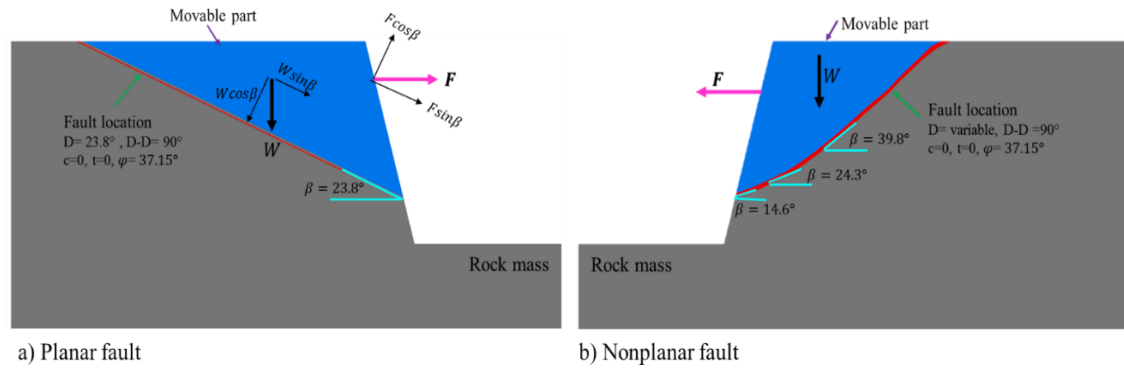


Fig. 3-7 Laboratory pull test procedure and parameters.

3.5. Results and Discussion

3.5.1. Analysis 1 (Fault geometry)

The sensitivity results of FOS values for planar, nonplanar, and undulated faults simulations are shown in Fig. 3-8. The results demonstrate high sensitivity of FOS for the UJ method for nonplanar geometry (about 35% higher than IF method). This is due to changes in the angle of discontinuity from 10° to 90° in the undulating faults; as explained earlier (Eq. (2.7) and (2.8)) for β less than the friction angle and β equal to 90° , failure cannot happen along the plane of weakness, and as a result UJ method shows artificially higher value of FOS. In addition, the results for undulating nonplanar and planar faults indicate the limitation of the UJ method in capturing the FOS because of the rapid change of β . The results show that the IF and Uj methods would have similar problems to simulate undulated fault shape. It seems that sliding cannot happen through the fault location.

The WZ method shows the expected increase of the FOS by increasing the irregularity of the geometry due to possible interlocking. The FOS was increased by 3% and 5% for undulating nonplanar and planar fault geometries, respectively. In contrast, the

IF method could not capture the correct trend, and the FOS values were decreased by 10% and 20% for undulating nonplanar and planar fault geometries, respectively.

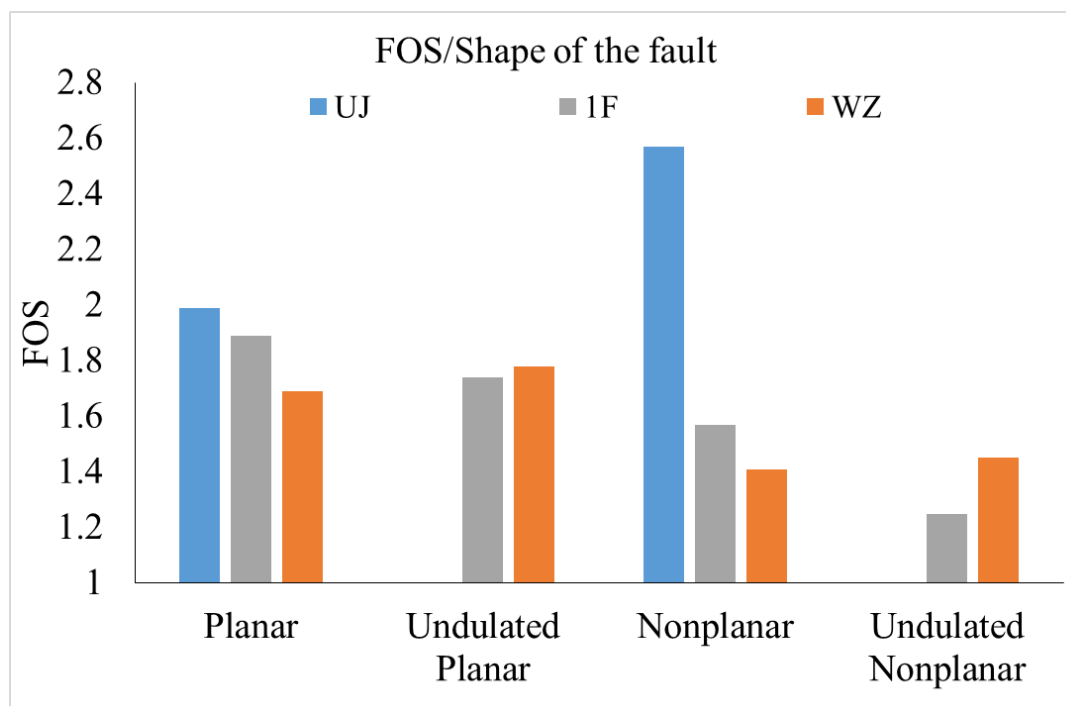


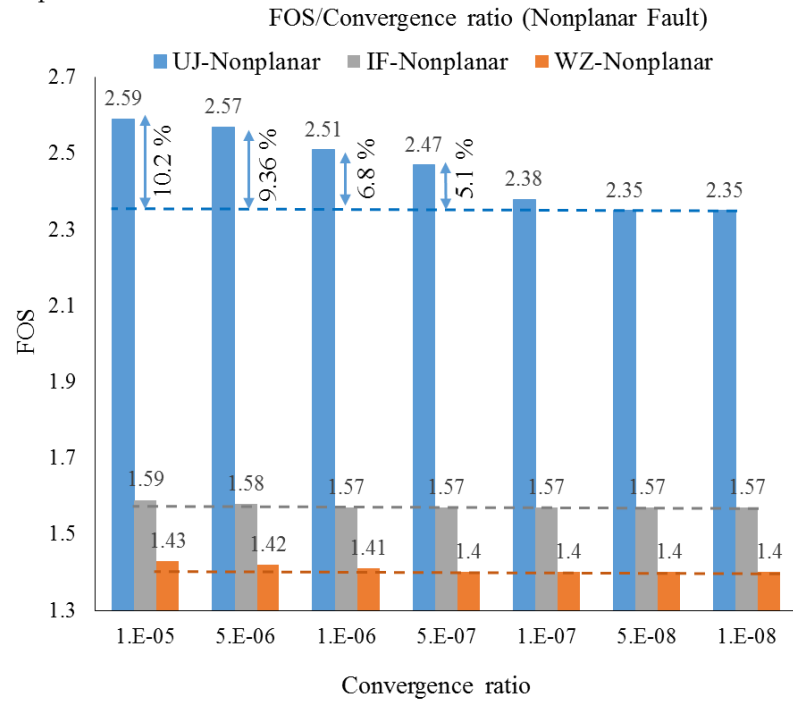
Fig. 3-8 Fault roughness effect on the FOS for weak zone (WZ), interface (IF), and ubiquitous joint (UJ) methods.

3.5.2. Analysis 2 (convergence ratio – numerical stability)

Fig. 3-9 shows the effect of changes in convergence ratio on the FOS values for the nonplanar and planar fault. The results indicate that in both planar and nonplanar faults, the FOS values reduce synchronously with decreasing the solve ratio (stronger convergence criteria). However, beyond a certain convergence ratio, below 10^{-7} , this change is negligible (less than 5%) in all three methods. The sensitivity of the IF and WZ methods regarding the convergence ratio is negligible; however, the UJ method shows

more sensitivity to the input solve ratios as it cannot capture the correct behavior of continuous features. The results for the nonplanar fault (Fig. 3-9, a) indicate that the optimum threshold for the convergence ratio is different for each method and by knowing this value it is possible to reduce computational cost and time without decreasing the accuracy of the results. In the case of planar faults (Fig. 3-9,b), none of the studied methods exhibit high sensitivity to the convergence ratio. It is concluded that the optimum threshold for the convergence ratio not only depends on the method of fault material simulation, but it also depends on the fault geometry.

a) Nonplanar fault



b) Planar fault

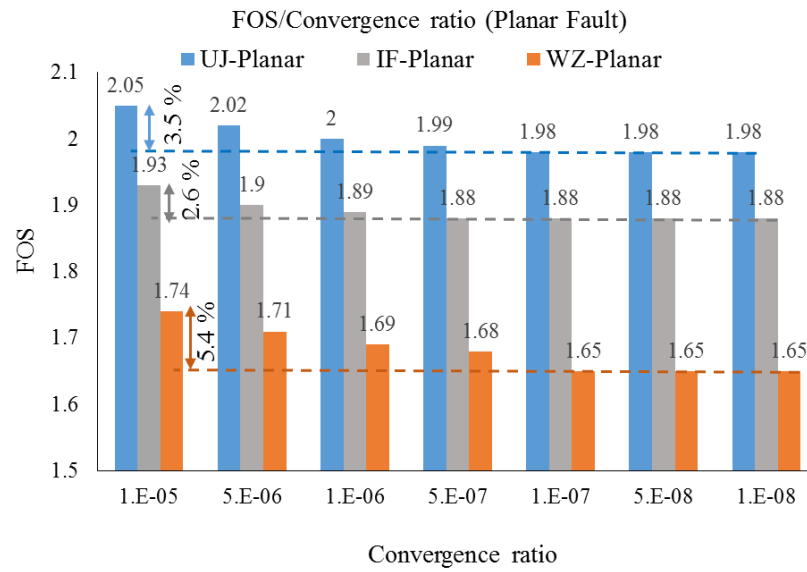


Fig. 3-9 Dependency of FOS on the convergence ratio, a) nonplanar fault, b) planar fault.

3.5.3. Analysis 3 (Mesh density)

The computational cost of increasing the mesh density scales as $\sim N^3$, where N is the number of nodal points (reference). In modeling a large scale open pit mine with several faults and geological features, increasing the number of nodal points (decreasing mesh size) to eliminate mesh dependency is practically impossible. For example, modeling half of an open pit mine with dimensions of 1000×500×400 m and mesh size of 4 m requires 3,125,000 elements, decreasing the mesh size to 2 m, which it is still not ideal, increases the number of elements to 25,000,000. Currently, no supercomputer can handle the calculation in a reasonable time.

The results of mesh density sensitivity analysis (Fig. 3-10) indicate that the FOS values are insensitive to the mesh density in the WZ method (the accuracy of FOS values improves by less than 5% by an \sim ten times increase in the mesh density.). However, this method is the most conservative technique (lowest FOS value) and low sensitivity to mesh size does not indicate the quality of the method. The IF method shows the median sensitivity (in comparison to the two other methods) regarding the mesh size (mesh density). The accuracy of FOS values improves by less than 5% by an \sim 10 times increase in the mesh density (Fig. 3-10). This is because the IF method relies on contact mechanics and it is mostly independent of the mesh density. The UJ method is the most sensitive, to the mesh density; the accuracy of its FOS values improves by \sim 31% with an \sim ten times increase in the mesh density. The UJ method only represents simple shear and not direct shear. In Fig. 3-10, the number of zones is an indicator of mesh density, as the dimension of the model is fixed (small scale). The expected error of FOS concerning the number of elements was

estimated based on the reliable threshold for all three methods (number of elements= 9000).

In addition, Fig. 3-10 shows that the optimum threshold for each method could be different.

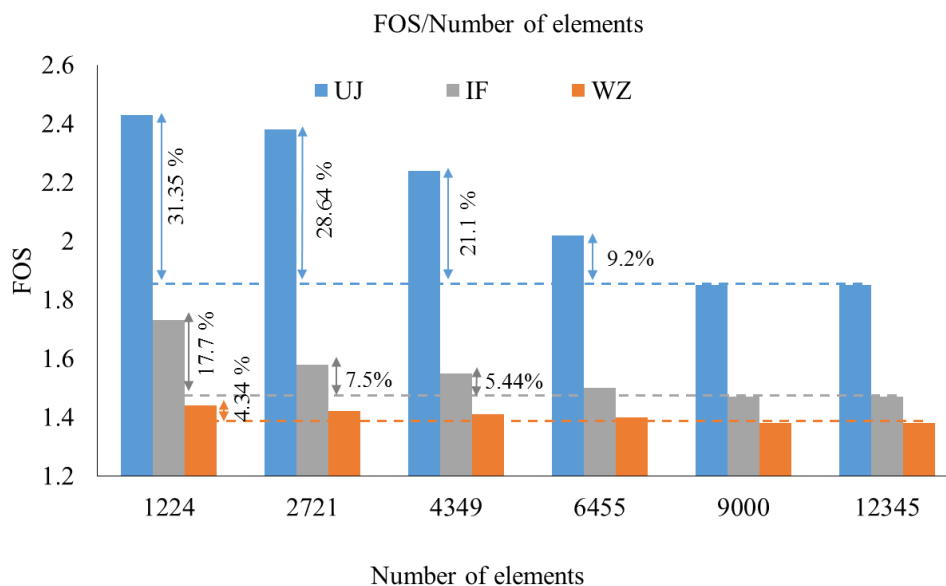


Fig. 3-10 Mesh density sensitivity analysis for the nonplanar fault.

3.5.4. Analysis 4 (Rock mass dilation)

The sensitivity of FOS values to variation of dilation angles (0-20 degrees) for the nonplanar fault is represented in Fig. 3-11. The results demonstrate that the FOS values are fairly independent of dilation angle in all methods. This is because the Mohr-Coulomb method applies the dilation properties only after failure (local or global). However, it can be argued that in a complex geotechnical model where a structure partially fails (weak materials fail but do not result in instability) the dilation would change the FOS value. The effect of dilation in such a scenario is beyond the scope of this study and requires future research.

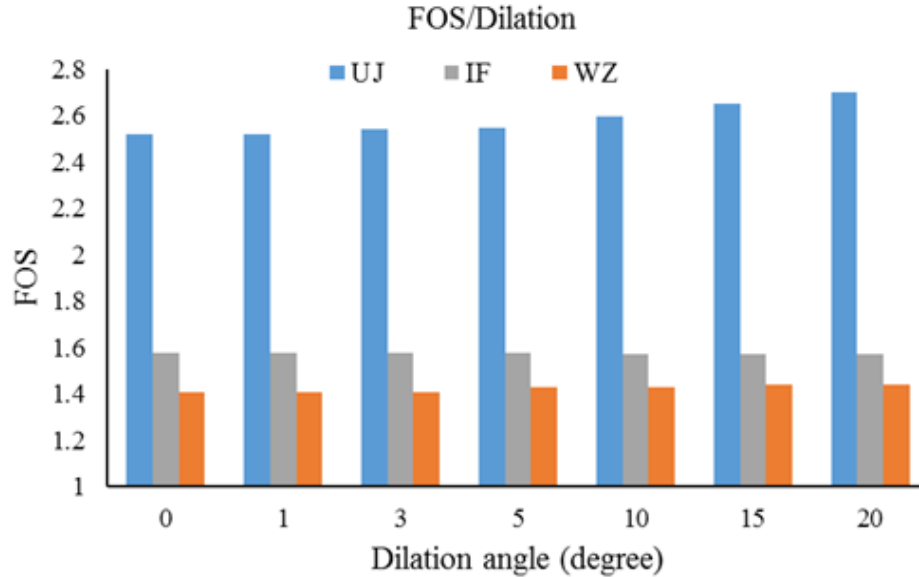


Fig. 3-11 FOS versus dilation angle for the nonplanar fault.

3.5.5. Analysis 5 (fault thickness)

The thickness of a fault plate is an important parameter for understanding the strength and fault behavior (displacement). The fault thickness can be varied from a few millimeters (clean face) to several meters with gouge and fill materials. Due to mesh size limitation (explained in mesh density analysis), it is difficult to capture the correct fault thickness in the modeling. In WZ and UJ method the minimum fault thickness can be one element, and in the IF method, the fault thickness cannot be represented.

The FOS results for different fault thicknesses are showcased in Fig. 3-12 for all methods other than IF; thickness does not apply to the IF method. As expected, the results show that increasing the fault thickness reduces the FOS obtained by all methods, although this reduction is less pronounced for the WZ method. Doubling the fault thickness from 1.5 to 3 meters decreases the FOS by approximately 13% in the UJ method. In this analysis,

the initial conditions are set in cautious proximity of imminent failure to compare the bare effect of each method. A more important result is that to capture a current behavior of the fault in WZ and UJ model a minimum of three elements is necessary along with the thickness of the fault (Fig. 3-13). One or two elements along the fault show a stiff structure that prevents the movement along the fault plane and unrealistically increases the strength. This is because in the continuum modeling the border fault elements are attached to the adjacent rock mass and the behavior of the elements is a product of the two systems (Fig. 3-13).

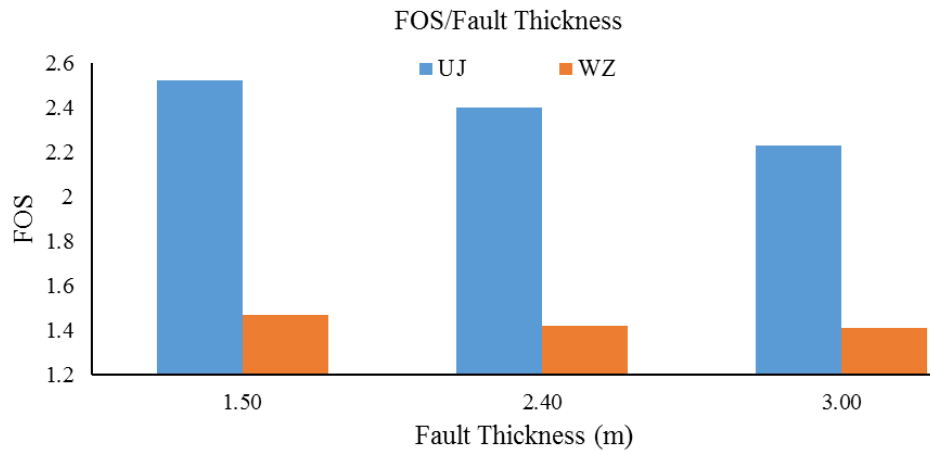


Fig. 3-12 FOS versus fault thickness for the nonplanar fault.

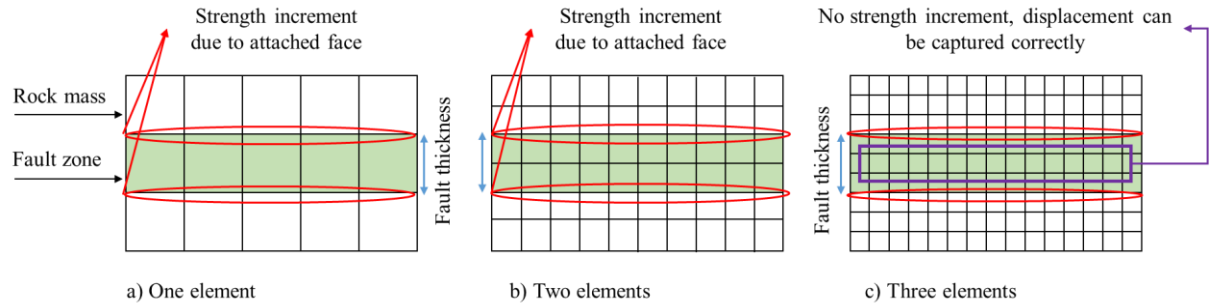


Fig. 3-13 Effect of the number of elements along the fault thickness (green zone): a) fault zone modeled with one zone, in this case the upper and lower nodes of the elements are connected to the rock mass and result in the fault having an unrealistic higher strength, b) fault zone modeled with two zones, in this case the upper and lower nodes of the fault boundary are connected to the rock mass and only the middle nodes are free to move along the fault, and c) fault zone modeled with three zones, in this case, the middle zone and nodes have enough degrees of freedom to move along the fault zone.

3.5.6. Analysis 6 (Fault shear strength)

A large source of uncertainty can be imposed on the design due to unreliable laboratory tests and lack of representative samples of the potential failure surface. Understanding the sensitivity of FOS value with shear properties of a fault is important in better understanding of the modeling result. The sensitivity of the FOS value in response to the changes in cohesion and friction angle (fault shear properties) is illustrated in Fig. 3-14 and Fig. 3-15, respectively. As in other analyses, the UJ method indicates the highest sensitivity. As expected, the FOS increases in tune with the increase of shear strength properties. However, this increment is more sensitive to cohesive properties (exponential dependency) of the fault material rather than its friction angle (linear dependency). This should be considered in the reduction methods, such as SSR, where cohesion and friction

angle are reduced by the same coefficient, whereas a lower coefficient should be given to the more sensitive property, i.e., cohesion. The high cohesion sensitivity and be explained using Eq 10, for shallow faults the confinement stress is low, and the effect of friction angle ($\sigma_n \tan \varphi_j$) is negligible, however, the reverse is true for deep fault with high confinement stress.

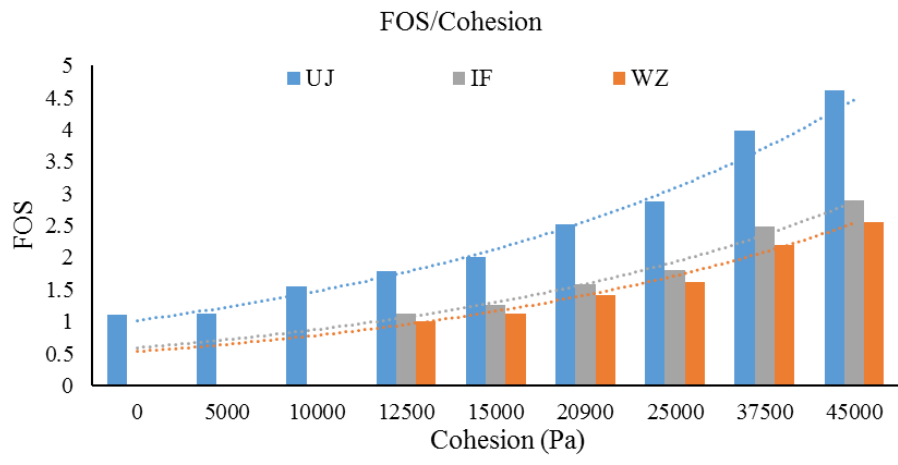


Fig. 3-14 FOS versus cohesion for the nonplanar fault.

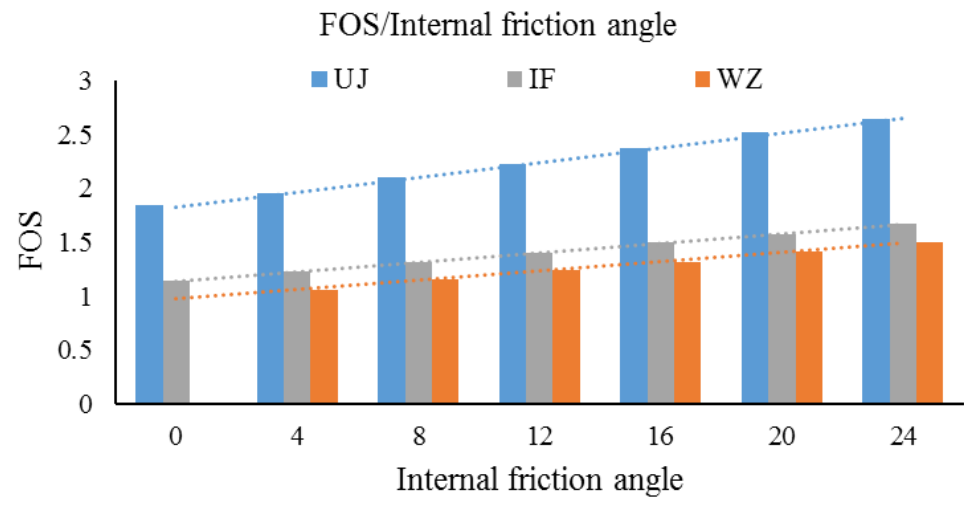


Fig. 3-15 FOS versus internal friction angle for the nonplanar fault.

3.5.7. Failure mechanism

In addition to the FOS, the failure mechanism encompasses important information about slope stability. Structural features, such as faults, and discontinuities form the plane of failure. Such surfaces usually are parallel or nearly parallel to the slope face. The sliding plane must daylight in the slope face or the plane should shear into the rock mass. The plane should also intersect the upper surface of the slope or form a tension crack to create a release backplane. Release surfaces that have negligible strength to sliding must be present in the rock mass to define the lateral boundaries of the slide. Capturing the correct failure mechanism requires a complex and accurate geotechnical and numerical model. The WZ, UJ, and IF introduce faults to the numerical model with different techniques, and this may result in capturing different failure surfaces. The failure mechanism predicted by each method (small-scale simulation) is shown in Fig. 3-16 for all fault geometries. Material properties for simulation are summarized in Table 3-1. Independent of the fault shape, tension and shear failures occur at the bench crest and toe, respectively, in the WZ (Fig. 3-16. a and b). In the UJ (Fig. 3-16. c and d) and IF methods (Fig. 3-16. e and f), however, shear failure is the dominant mechanism throughout the fault. These methods capture the failure mechanism more accurately. Nonetheless, our experience and results imply that the fault modeling methods are intrinsically different, and each suffers from a different set of limitations, making the mechanistic investigations more challenging.

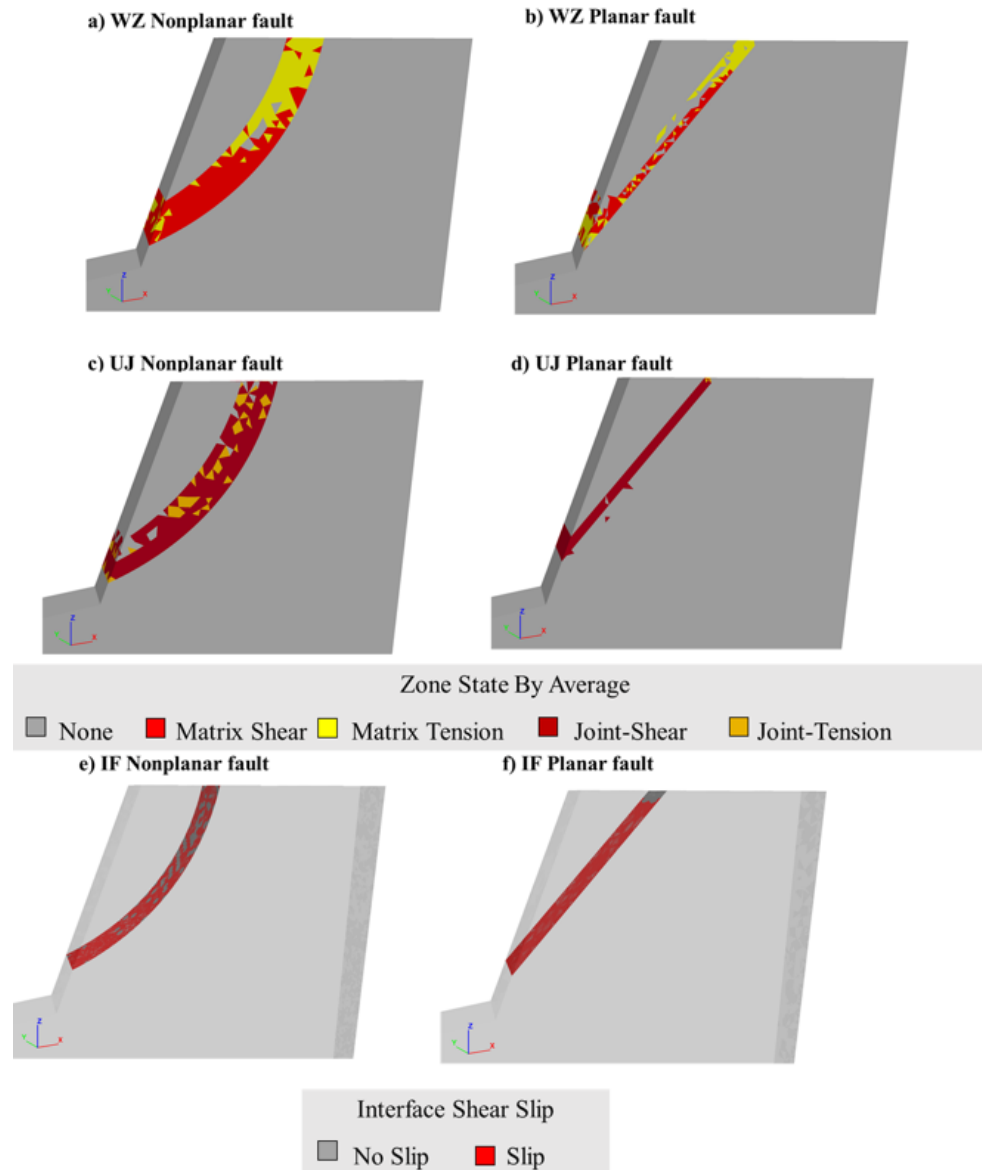


Fig. 3-16 Failure mechanism of a) WZ nonplanar, b) WZ planar, c) UJ nonplanar, d) UJ planar, e) IF nonplanar, and f) IF planar faults.

3.5.8. Large Scale Results

The proper modeling of the fault by the IF is quite challenging in the large-scale; however, the faults in the whole open pit mine are modeled using WZ and UJ methods (Fig. 3-17 and 20). The large-scale model is built based on findings and considerations

attained by the small-scale modeling. Similar to the small scale case, applying the UJ method results in higher values for the FOS (2.18) compared to the WZ method (1.38). The difference between FOS value for WZ and UJ is 36% and 15% for large scale and small scale, respectively. The variation of FOS value for bench scale model (small model) is negligible, but it is not within the acceptable range of error for the large scale model. This shows that selecting an appropriate modeling technique is critical for large open pit mine modeling. Fig. 3-17 and 19 show the displacements in the fault zone modeled by WZ and UJ methods, respectively. As it is deduced from the FOS values, UJ model has higher displacements, but both WZ and UJ models have their maximum displacements at the toe of the fault. This can imply that the failure initiates at the bottom of the fault, and both shear and tension participate in the failure mechanism. This failure mechanism is better captured in Fig. 3-19 (WZ) and Fig. 3-20 (UJ); in both, shear is dominant in the fault zone (slipping along fault plane). Massive tension failure is shown in the WZ model within the mobilized rock mass. Similar to the small scale model, this can be an indicator of toppling failure, which is not realistic.

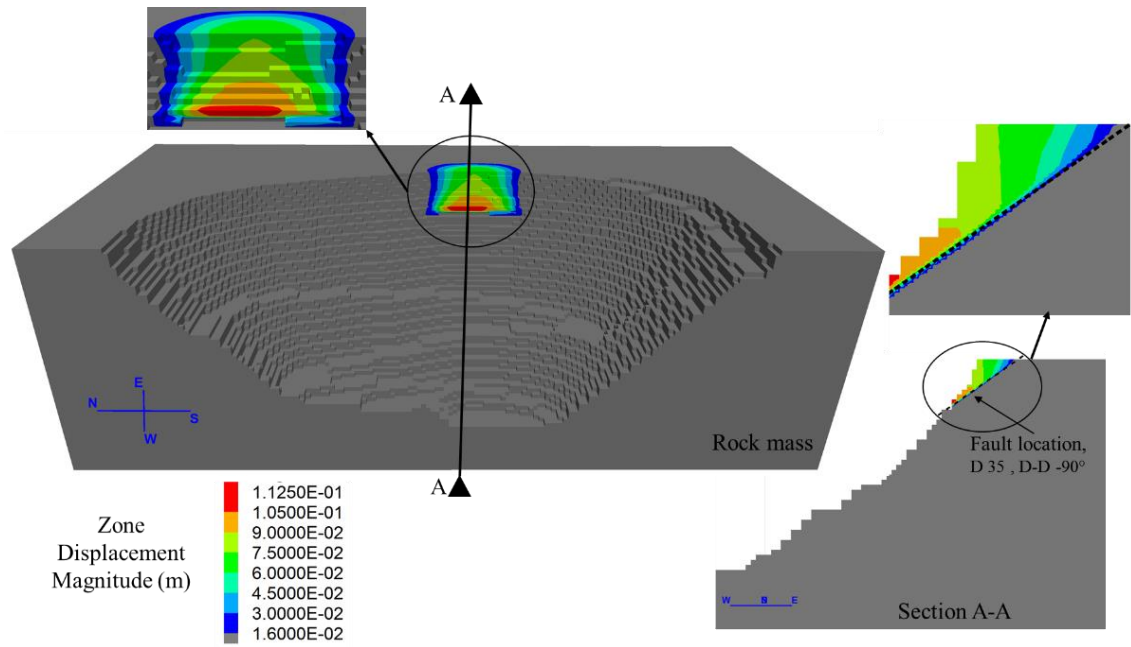


Fig. 3-17 Displacement contours, using the WZ method. The black dashed line demarcates the fault location.

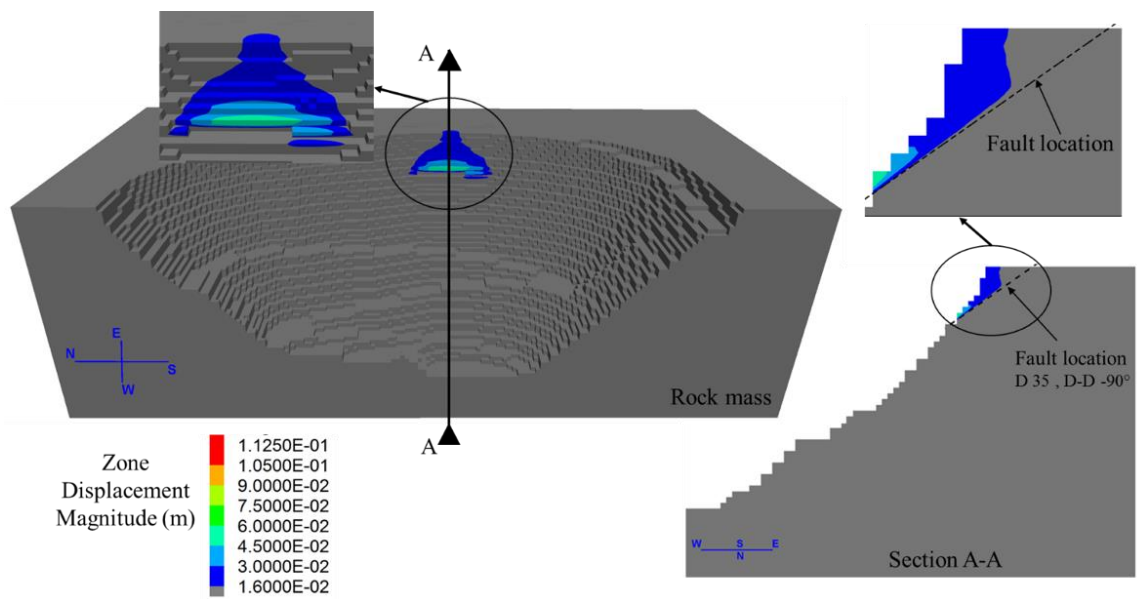


Fig. 3-18 Displacement contours, using UJ method. The black dashed line demarcates the fault location.

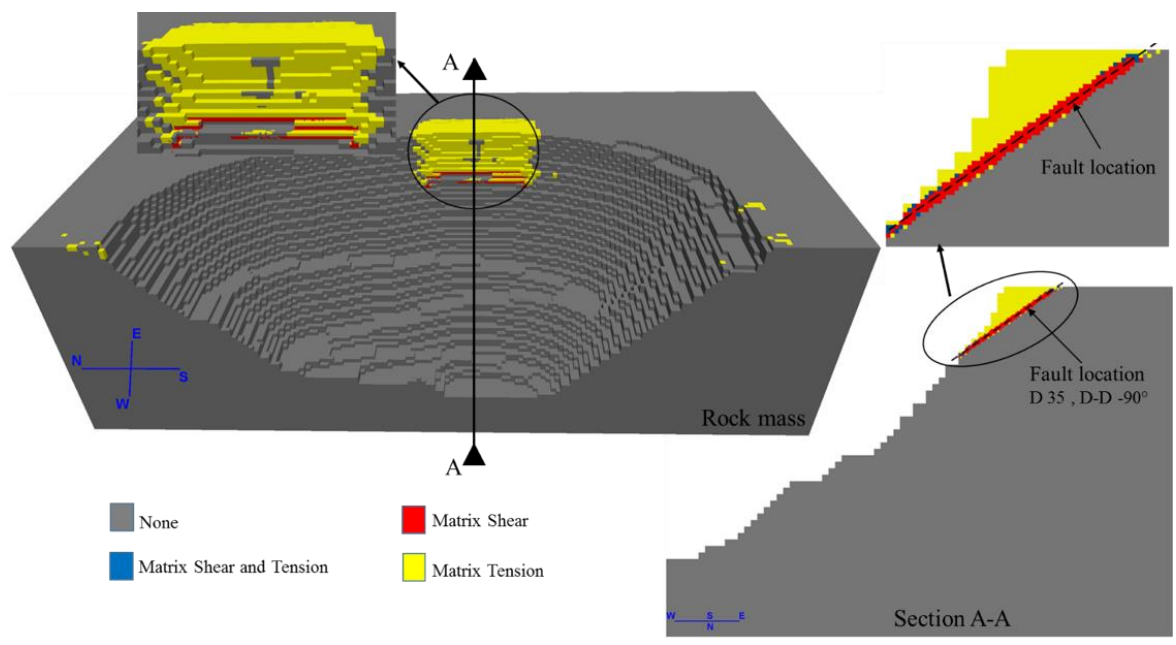


Fig. 3-19 Failure mechanism obtained by the WZ method. The black dashed line demarcates the fault location.

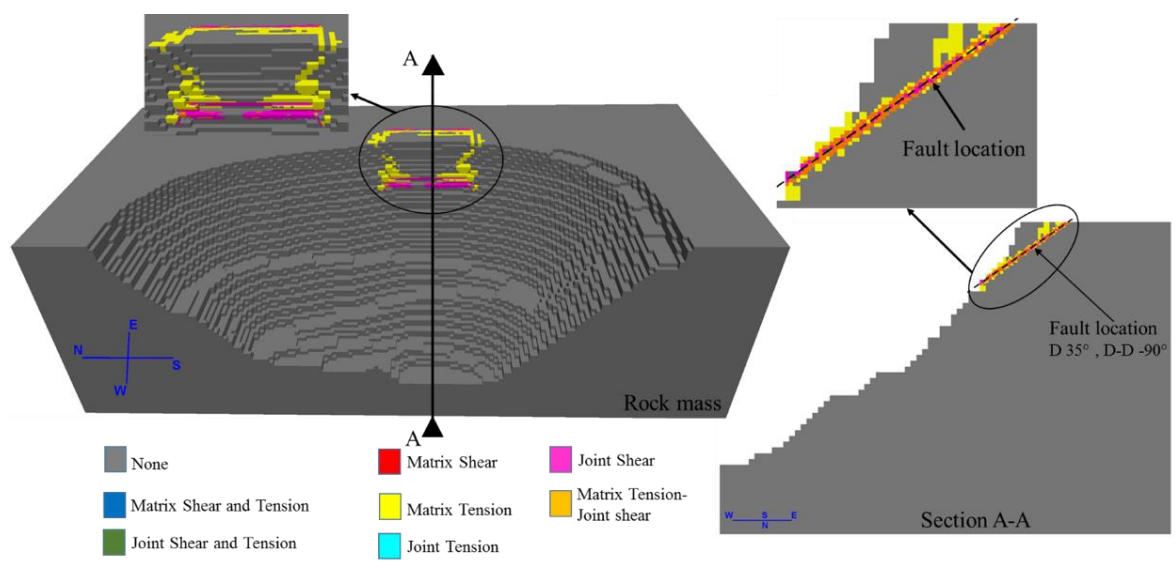


Fig. 3-20 Failure mechanism obtained by UJ method. The black dashed line demarcates the fault location.

3.5.9. Laboratory Results

The median value of friction angle of the laboratory models with the planar fault (STDEV = 0.549 for 90 measurements) is 37.15 degrees. With this friction angle and dip angle of 23.8 degrees, the FOS is 1.718 using Eq. 13. An identical geometry and material properties were used to simulate the laboratory test model in FLAC3D software. It should be mentioned in this experiment, fault material was considered as non-cohesive material. A comparison between this FOS value and those of scanned model (FOS_{WZ} = 1.51, FOS_{IF} = 1.62, and FOS_{UJ} = 1.76) indicates a good agreement between the UJ and IF methods and the laboratory model (~3-5% discrepancy, Table 3-2). This agreement is not surprising, as all properties of the laboratory model are exactly transferred to the software, including zero cohesion for the fault zone. Calibration between the median force obtained from the pull test of the planar laboratory model and the force required for imminent failure from Eq. 14 results in a 0.925 correction factor (STDEV = 0.864 for 134 measurements). Also, a comparison between the median force obtained from the pull test of the nonplanar laboratory model (normalized by correction factor) and the loading forces of scanned models indicates that IF and UJ methods are more successful in modeling the failure for non-cohesive faults. These values are 11.90, 10.75, 11.5, and 12.12 N for the normalized median pull force, and the loading forces from WZ, IF, and UJ models. The summary of the result is shown in

Table 3-3. More laboratory tests are needed for cohesive material and large-scale model.

Table 3-2. Summary of the calculated FOS for planar sample

	Numerical modeling			Laboratory
	WZ	IF	UJ	Analytical
FOS	1.51	1.62	1.76	1.71
Error (%)	-11.7	-5.27	2.93	N/A

Table 3-3. Summary of the pull test results for the nonplanar sample

	Numerical modeling			Laboratory
	WZ	IF	UJ	Direct measurement
Force required for imminent failure (N)	10.75	11.5	12.12	11.9
Error (%)	-9.67	-3.37	1.85	N/A

Acknowledgment:

The material of present chapter has been submitted for publishing in the “Rock Mechanics and Rock Engineering” journal with the title of “Structure Stability Analysis of Rock Structure in Open-Pit Mine: Numerical and Experimental Fault Modeling”. The author would like to thank the co-authors of paper Dr. Seyedsaeid Ahmadvand and Dr. Behrooz Abbasi for their contribution.

Also, the result of sensitivity analysis for small scale simulation (one bench of open-pit mine) has been published in "52nd US Rock Mechanics / Geomechanics Symposium, 2018" with the title of "A Discussion on Numerical Modeling of Fault for Large Open Pit Mines." The author would like to thank the co-authors of paper Mr. Bijan Peik, Dr. Behrooz Abbasi and Dr. Pedram Roghanchi for their contributions.

4. Chapter 4 – Effect of Hydro-Jex Operation on the Stability of Heap Leach Pads: A Case Study of the Los Filos Mine, Mexico ¹

4.1. Introduction

The Los Filos Mine is one of the largest gold mines in Mexico, being commercially operated for a decade. The Mine consists of two open pits and one underground mine, sharing the heap leach, wet plant, and ancillary facilities (Reddy, et al., 2018). Hydro-Jex technique with 16 wells was designed, drilled, and equipped at the Los Filos Mine, allowing for the injection of 59,000 m³ of the barren fluid to material columns. This put nearly 800,000 metric tons of previously leached ore in contact with fresh chemicals and swept the dissolved gold to the drainage system. Around 15 meters safety distance was utilized between the bottom of the wells and the liner to reduce any possible damage to the liner during drilling. Before installing the perforated wells for injection, surface irrigation was withheld from the area to be targeted, thereby allowing drainage of the heap for several weeks. The procedure used a packer system in the casing such that the fluid was only

¹ this chapter of thesis has been submitted in the “Mining, Metallurgy & Exploration” journal with the title of “The Effect of Hydro-Jex Operation on the Stability of Heap Leach Pads: A Case Study of the Los Filos Mine, Mexico”.

applied to a single zone within the perforated casing. The fluid injection zone was then relocated to another perforated zone, or another well if the initial zone was sufficiently stimulated or pumped.

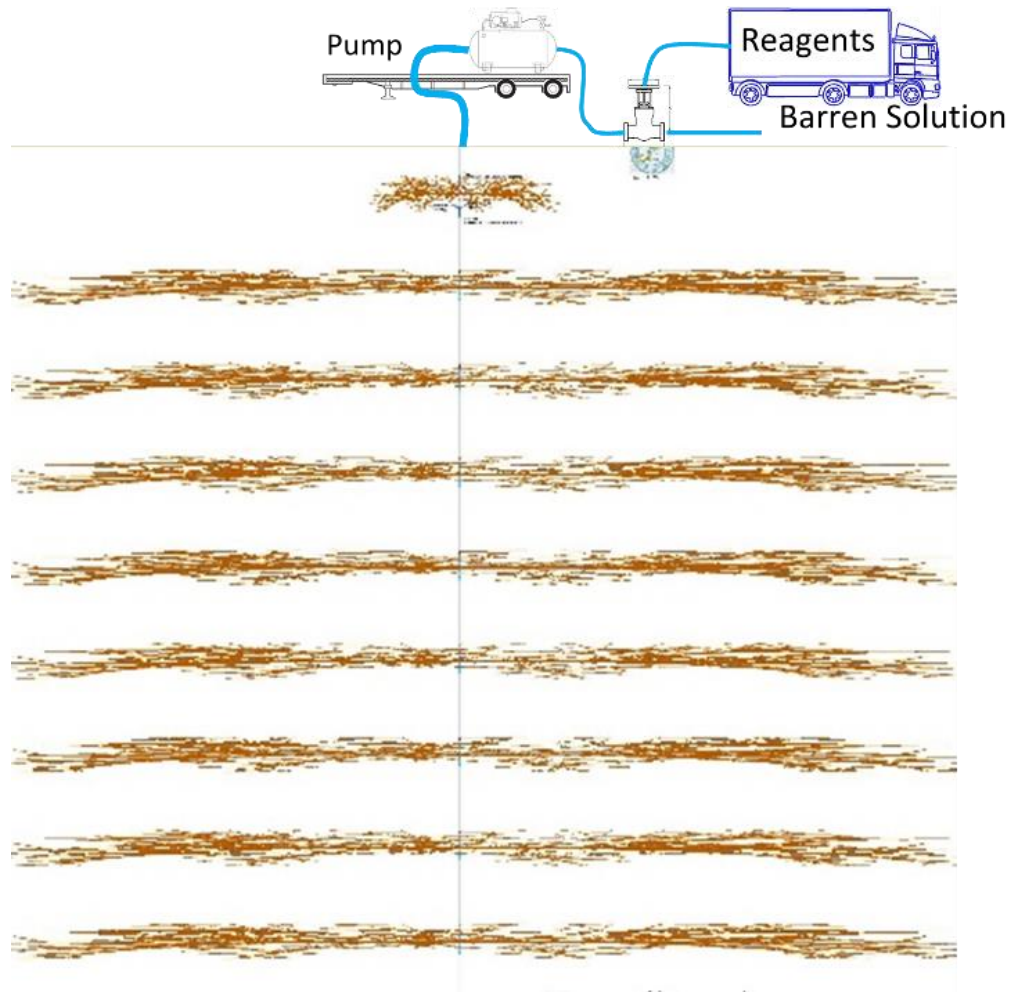


Fig. 4-1. Drawing of zones impacted by the pumping of the solution down a perforated Hydro-Jex[®] well

4.2. Model Development

The fast Lagrangian analysis of continua in 3-dimensions (FLAC3D) software was used to build a 3-D model of the heap structure. The as-built data of the installed liner and

topography of the heap leach surface were used to build the model to real conditions within reasonable accuracy. The well-monitoring results and geophysical data were applied to define the phreatic surface and pore pressure (Fig. 4-2 and Table 4-1). Fig. 4-4 shows the pore pressure among the model and across the electrical resistivity survey lines based on the phreatic surface derived from geophysical data. The model dimensions were set to $900 \times 800 \times n \text{ m}^3$, n being the adjustable height based on the actual topography (Fig. 4-3). The bottom and faces (West-East and North-South faces) of the model were constrained in a normal direction to achieve a more realistic displacement. The slope strike is north-south, the dip direction is the east-west direction, and dip angle of the face slope is 35 degrees. A thin layer (one-meter thickness) with an adequate value of cohesion was defined to prevent any failure at the surface. Also, the Hydro-Jex wells were introduced to the model as piles. The pile element is a structural element that is defined by geometric, material and coupling-spring properties (Table 4-2). It acts like a structural-support, and the frictional interaction occurs between the pile and the rock or soil mass in the normal and shear-directed, perpendicular and parallel to the pile axis respectively (Itasca, 2017).

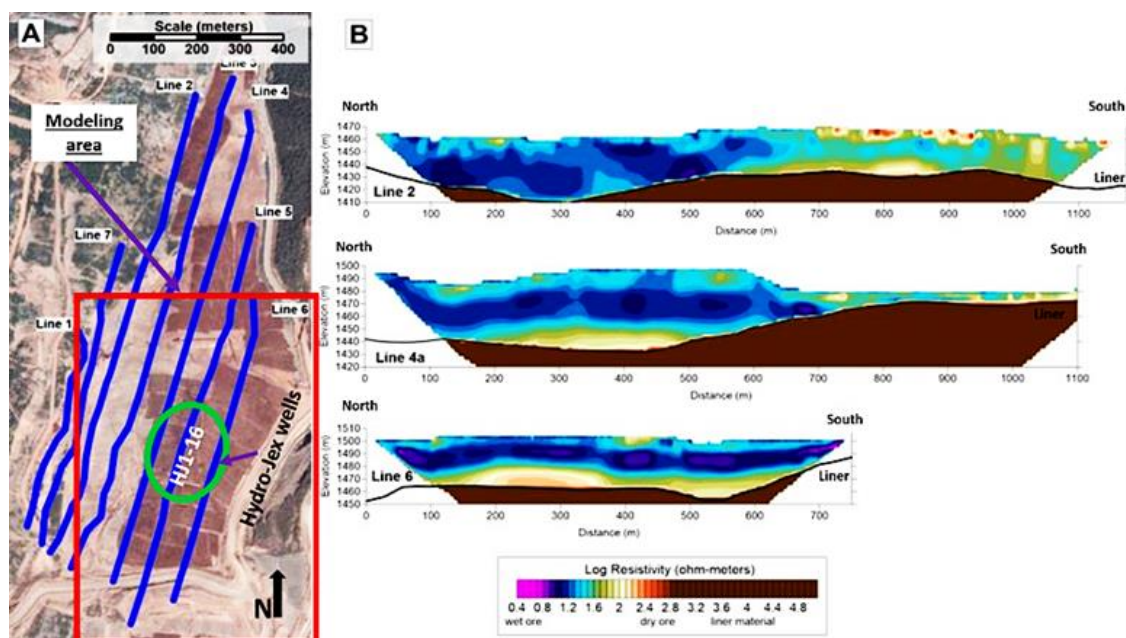


Fig. 4-2. Electrical resistivity survey across a leach pad at the Los Filos Mine used to build the phreatic surface and pore pressure in numerical modeling. A) Survey line locations, B) Results of three resistivity lines (Basi, et al., 2017)

Table 4-1. Wells monitoring results before stimulation.

Hole #	Surface Elev.(m)	Liner Elev.(m)	Max Hole Depth (m)	Solution Elev.(m) *	Solution Depth to Liner(m)
HJ-1	1,506	1,439	55	1496.2	53.2
HJ-2	1,506	1,445	49	1,493	48
HJ-3	1,501	1,444	43	---	---
HJ-4	1,500	1,444	43	---	---
HJ-5	1,507	1,448	43	1499.2	51.2
HJ-6	1,506	1,450	43	1496.7	46.7
HJ-7	1,507	1,456	37	1496.4	40.4
HJ-8	1,507	1,461	31	1497.4	29.4
HJ-9	1,507	1,468	25	1498.9	30.9

Hole #	Surface Elev.(m)	Liner Elev.(m)	Max Hole Depth (m)	Solution Elev.(m) *	Solution Depth to Liner(m)
HJ-10	1,507	1,474	19	1501.9	27.9
HJ-11	1,506	1,447	43	---	---
HJ-12	1,507	1,455	37	---	
HJ-13	1,507	1,449	43	1500.1	51.1
HJ-14	1,506	1,460	31	---	---
HJ-15	1,507	1,467	25	1494.4	27.4
HJ-16	1,507	1,466	25	1494.7	28.7

*The phreatic surface elevation before the Hydro-Jex operation. After the operation, no water observed in any of the wells.

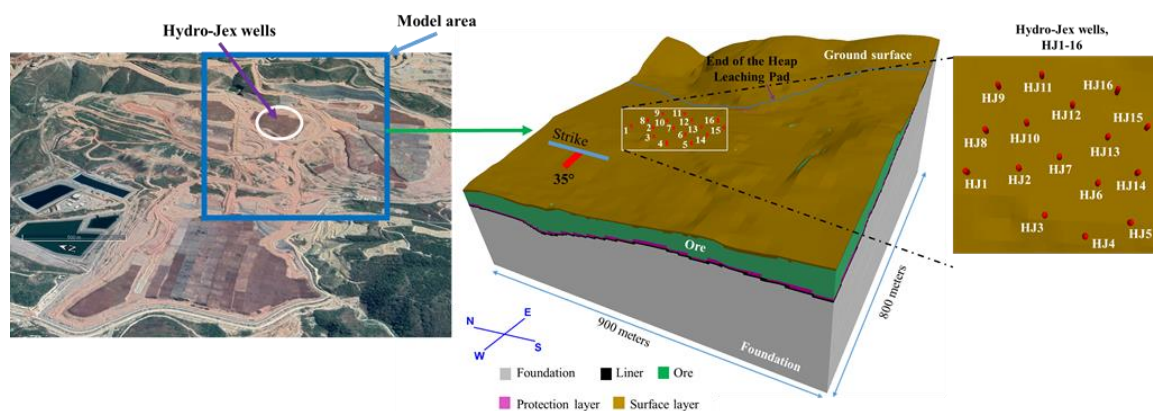


Fig. 4-3. The model geometry and location of Hydro-Jex wells.

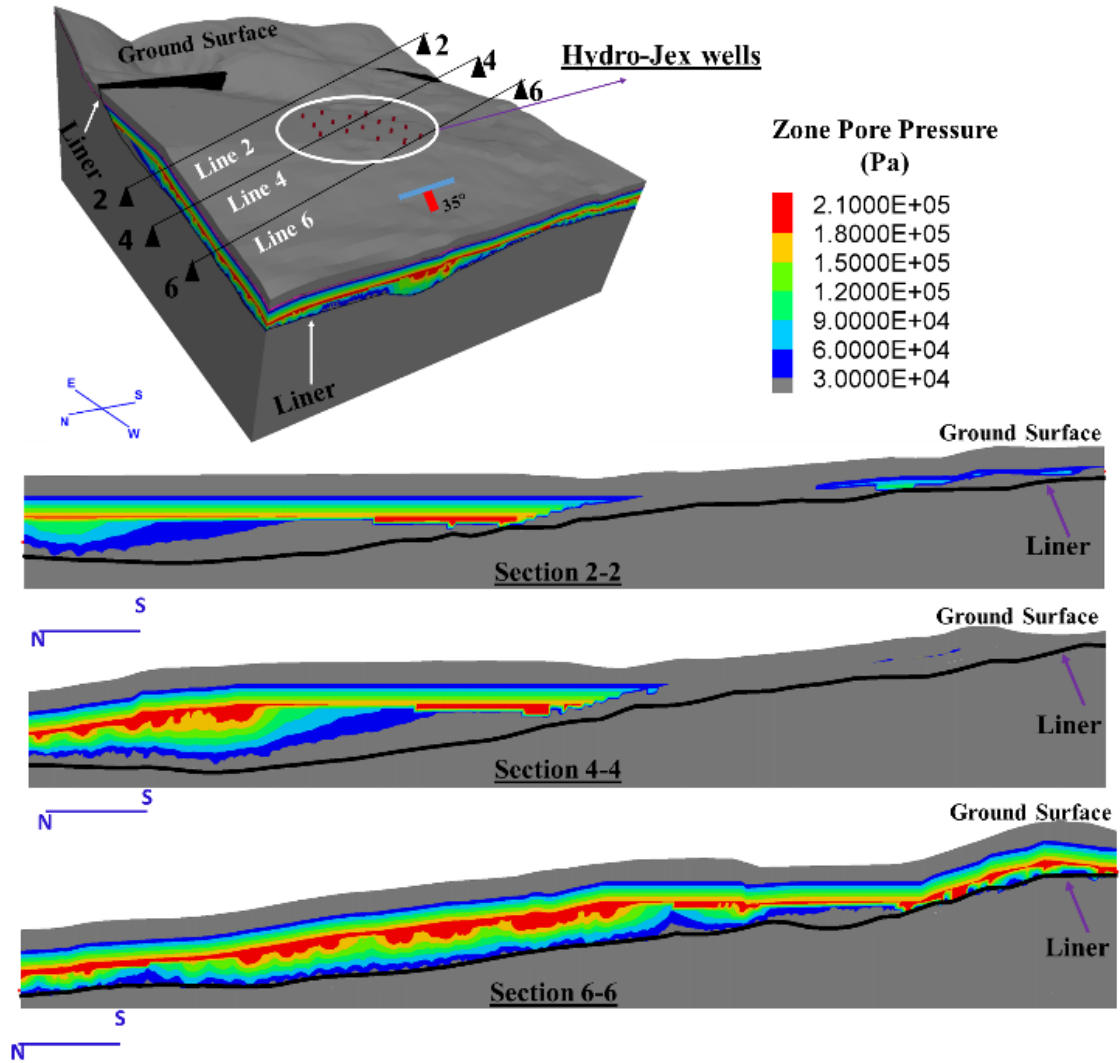


Fig. 4-4. Pore pressure counters in the model and across the electrical resistivity survey lines. The black line shows the liner location.

Table 4-2. Pile properties for the numerical modeling

Material properties	Quantity
Cross-sectional-area	0.0182 (m ²)
Perimeter	0.47854 (m)
Young's modulus	20×10^{10} (Pa)
Poisson's ratio	0.3
Coupling-stiffness-shear	1.3×10^{11} (Pa)
Coupling-cohesion-shear	1.0×10^{10} (Pa)
Coupling-friction-shear	36 (Degree)
Coupling-stiffness-normal	1.3×10^9 (Pa)
Coupling-cohesion normal	1.0×10^4 (Pa)
Coupling-friction-normal	10 (Degree)

The brick element was used to create complex geometries in the mesh design. Also, to obtain more volumetric flexibility and fluidity for plasticity analysis, the nodal mixed discretization (NMD) technique was used (Abbasi, et al., 2013)

For modeling the heap leach, elastic-plastic material was chosen, in which the Mohr-Coulomb failure criterion is met. Foundation properties were considered as limestone to prevent movement or cracking of the liner under the heap weight or geological

conditions of the site. Based on the available grain size distribution analysis, the heap material was divided into two major groups. Ore material and protection layer were introduced as gravel and sand materials, respectively. The properties of the heap material were defined and reported in Table 4-3. Also, a thin layer with minimum cohesion was deposited to the surface to prevent any immediate surficial failure.

Table 4-3. Material properties for the numerical modeling

Material properties	Foundation	Ore	Surface layer	Protection layer	Liner	Unit
Density	2500	2000	2000	1800	600	kg/m ³
Bulk modulus	10×10^9	80×10^6	80×10^6	27.7×10^6	3.45×10^9	Pa
Shear modulus	4.6×10^9	48×10^6	48×10^6	11.36×10^6	3.57×10^8	Pa
Cohesion	5×10^6	0	2×10^5	0	--	Pa
Tension	5×10^5	0	2×10^4	0	2×10^6	Pa
Internal friction angle	36	33	33	32	14	Degree

The shear strength reduction method (SRM) was used to calculate the FOS for slope stability. In the SRM approach, the actual shear strength properties (cohesion, internal friction angle, and tension) of the various units were reduced by the strength reduction factor (SRF) until failure (Fig.2-1, (Dawson, et al., 1999)).

$$FOS = SRF = \frac{C_0}{C_r} = \frac{\tan \varphi_0}{\tan \varphi_r} \quad (4.1)$$

In Eq. 4.1, C_0 , C_r , $\tan \varphi_0$, and $\tan \varphi_r$ are initial and reduced cohesive strength and initial and reduced internal friction angle, respectively and the FOS and SRF are equal.

From a geotechnical point of view, the predominant concern of using the Hydro-Jex technology is related to the change of stress distribution on the heap leach pad. Due to the drag forces induced by the high-pressure injection, the particulate tends to move away from the injection point, leaving a near horizontal voidage channel behind. Also, it causes the finer-grained materials to move out of the area near the well (Fig. 4-5, (Basi, et al., 2017)). Horizontal cavity creation and fine grain washout near the wellbore increase the permeability of heap materials after the short-term pumping of several hours, allowing the solution to return to the perforated wellbore then down to the bottom of the well and consequently, the phreatic surface will drop down and drain. This eventually affects the pore pressure and stress distribution.

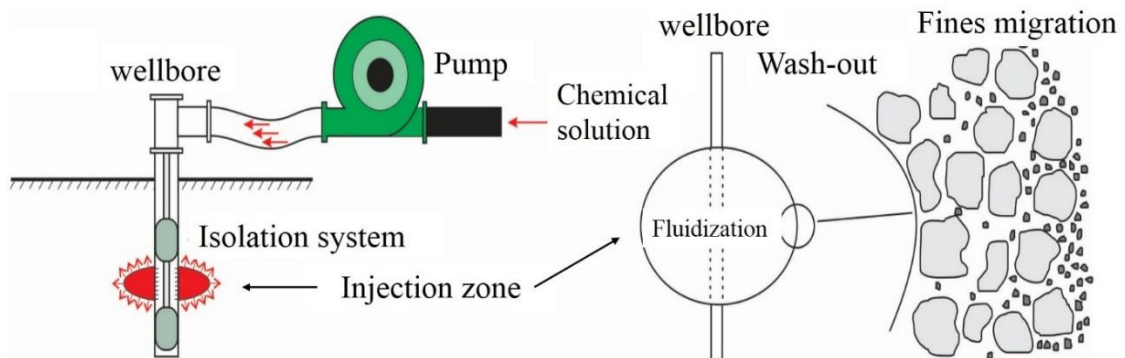


Fig. 4-5. The schematic representation of cavity initiation and washout of fines near the wellbore

(Basi, et al., 2017)

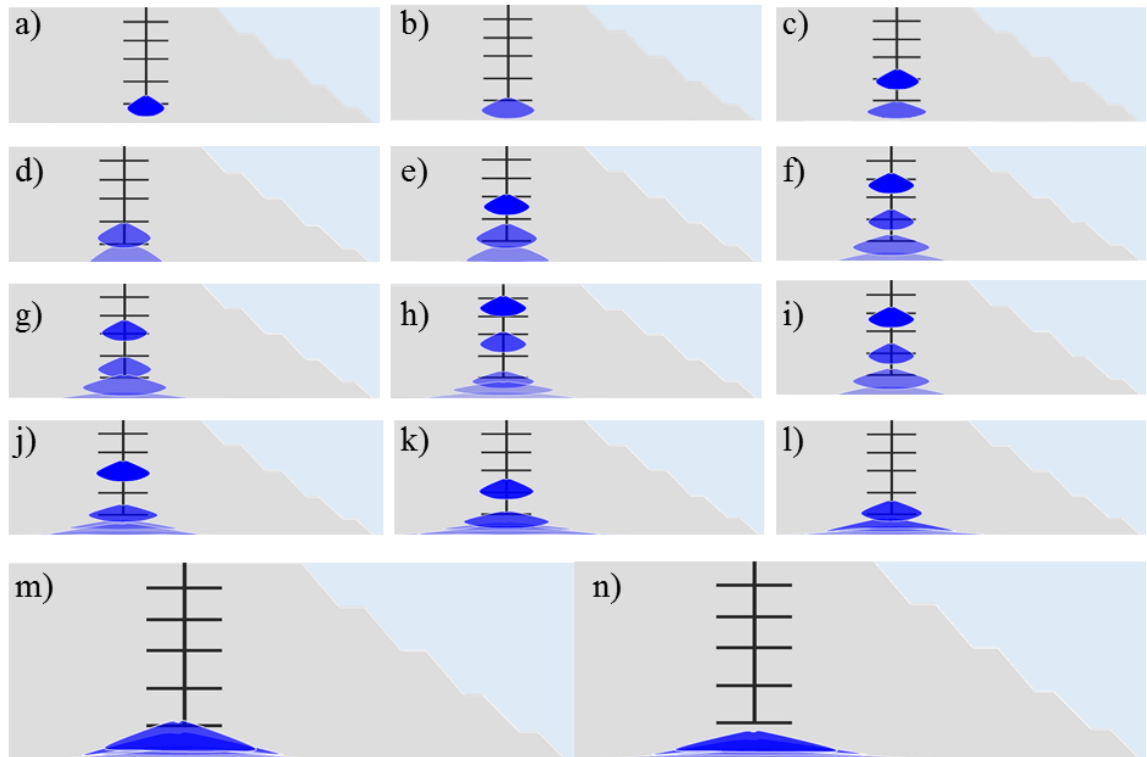


Fig. 4-6. The schematic treatment (a to n) and drain down from each zone in a Hydro-Jex® well-pumping stimulation (Kunkel, 2009)

The FOS is defined as the ratio between the shear strength and stress required for equilibrium (Bishop, 1955). Using Mohr-Coulomb's criterion for failure (Eq.4.2,) and Terzaghi's expression for effective stress (Eq.4.3); the FOS can be defined as (Hopkins, et al., 1975):

$$\tau = c + \sigma \tan \phi \quad (4.2)$$

$$\sigma' = \sigma - u \quad (4.3)$$

$$\begin{aligned} \text{FOS} &= \frac{\text{shear strength of soil unit}}{\text{shear stress required for equilibrium}} = \frac{c + \sigma \tan \varphi}{\tau} \\ &= \frac{c + (\sigma - u) \tan \varphi}{\tau} \end{aligned} \quad (4.4)$$

where τ is the shear stress on the failure plane, c is the cohesion, σ is the total normal stress on the failure surface, φ is the angle of internal friction, σ is the effective stress, and u is the pore pressure. In the numerical approach (Finite difference -FLAC3D), the tetrahedron nodes are referred by number 1 to 4, and fluid density and pore pressure are assumed constant and linear within a tetrahedron, respectively. The Gauss divergence theorem is used to find the pressure head gradient (Itasca, 2017),

$$(p - pf x_i g_i)_j = -\frac{1}{3V} \sum_{l=1}^4 (P^l - pf x_i^l g_i) n_j^{(l)} S^{(l)} \quad (4.5)$$

where n^l is the exterior unit vector normal to face l , S is the face surface area and V is the tetrahedron volume. To increase the numerical accuracy, x_i is substituted by $x_i - x_i^1$ in Eq.4.5 that x_i^1 corresponds to the coordinates of one of the tetrahedron's corners. As a result, Eq.4.5 can be replaced by (Itasca, 2017):

$$(p - pf x_i g_i)_j = -\frac{1}{3V} \sum_{l=1}^4 p^{*l} n_j^{(l)} S^{(l)} \quad (4.6)$$

where the nodal quantity p^{*l} is defined as,

$$p^{*l} = p^l - pf(x_i^l - x_i^1) g_i \quad (4.7)$$

4.3. Results And Discussion

One way to investigate the stability of the Hydro-Jex operation is to compare the phreatic surface before (conventional heap leaching) and after injection. Such a comparison shows that the Hydro-Jex operation reduces the saturation zone and thus the phreatic surface goes below the wellbore bottoms (Table 4-1) in the long run. Lowering the water table level decreases the pore pressure and increases the FOS. Ideally, using an optimum-pressure injection increases the permeability of the heap and keeps the solution from aggregation anywhere above the liner. This pressure should be high enough to increase the zone permeability, of the short time duration of a few hours, to expedite the leaching time and low enough not to risk the stability of the heap. Overburden pressure, at the level of injection, is usually less than the lower limit to lift the above material up and it increases effective permeability. As the saturation level drops below the wellbore depth, the situation after the Hydro-Jex operation can be considered as a drain downstate. For the modeling purpose, only static conditions were considered. A series of stability analyses have been conducted to evaluate the stability of saturated and dry conditions before and after Hydro-Jex operation. A higher value of FOS is an indicator of higher general stability of the heap leach pad at each stage. The modeling results show the FOS values of 3.35 and 2.68 for the dry (after Hydro-Jex) and saturated (before Hydro-Jex) conditions, respectively. This implies that the Hydro-Jex operation improves the stability of the heap leach pad by 26% at the Los Filos Mine. Fig. 4-7 and Fig. 4-8, show the maximum displacement before and after Hydro-Jex operation, respectively. Drainage of the fluid leaves no pore pressure after the operation; however, overburden pressure is still present in all cases. After the Hydro-Jex (Fig. 4-8) injection in wellbore HJ.6 (Hydro-Jex well number 6), the depth of mobilized

zone and magnitude of displacement around the HJ.6 reduces by 50 percent (from 27 m to 13 m) and 28 percent (from 14 cm to around 10 cm), respectively. This can be referred to as an increase in permeability followed by a decrease in pore pressure after the operation. Also, steel casing installed in the wellbore acts similar to reinforcement with soil nails. Precise measurement and modeling of permeability of the in-situ material can further support these results.

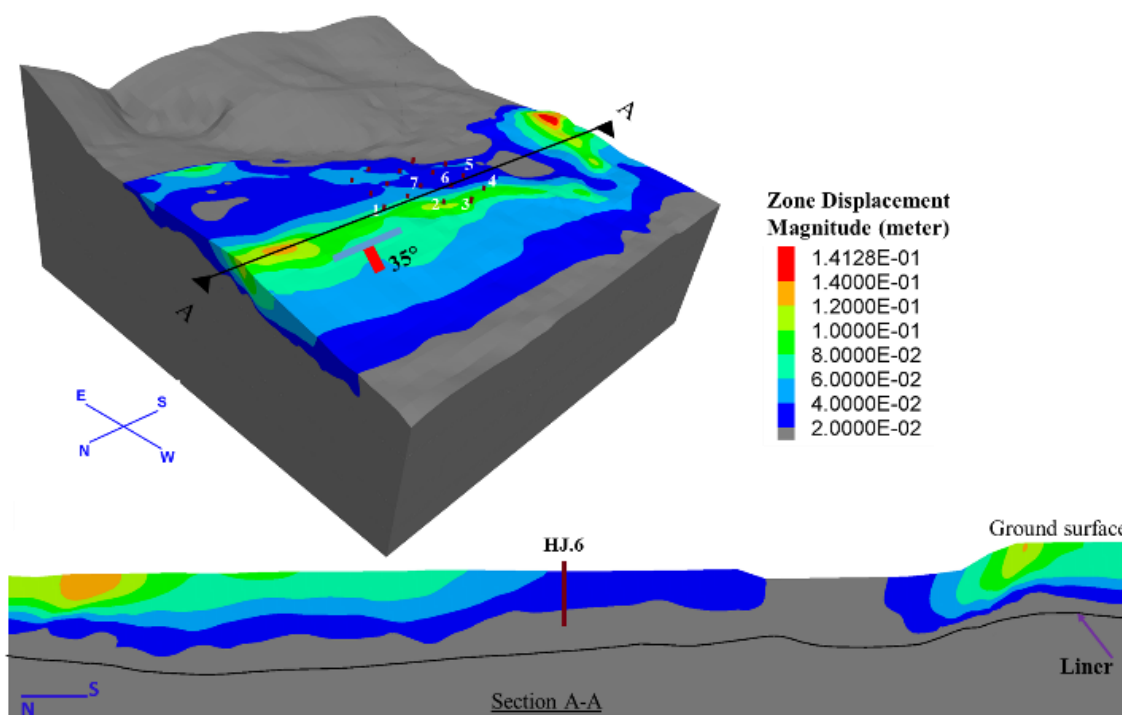


Fig. 4-7. Displacement before the Hydro-Jex operation at the heap leach pad. The black line demarcates the liner location.

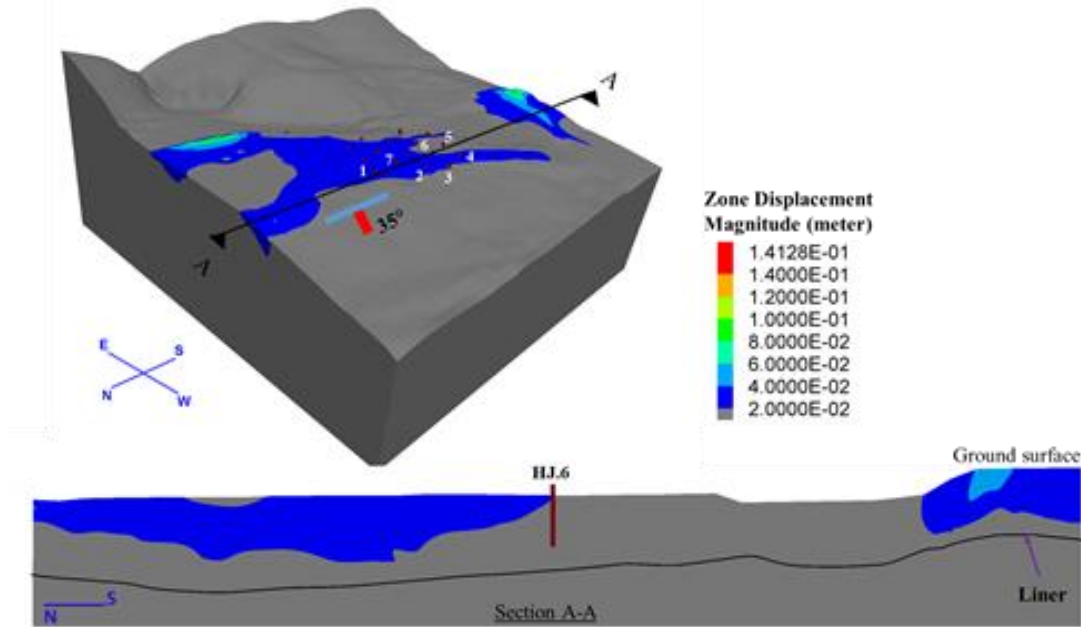


Fig. 4-8. Displacement of the heap leach pad after the Hydro-Jex operation. The black line demarcates the liner location.

Fig. 4-9 illustrates a sensitivity analysis on the impact of the phreatic surface depth on the stability of the heap leach pad. As the phreatic surface depth increases, the FOS and thus stability increases. However, the FOS value for the phreatic surface of 20 m below the ground surface (about one-third of liner depth) and the dry condition is 3.3 and 3.4, respectively, which shows a less than 3 percent increase. Fig. 4-10 shows the displacement in the heap leach pad as a function of the phreatic surface depth. The results show that the maximum displacement in the heap leach pad is reduced from 17 cm to 4 cm by increasing the phreatic surface depth.

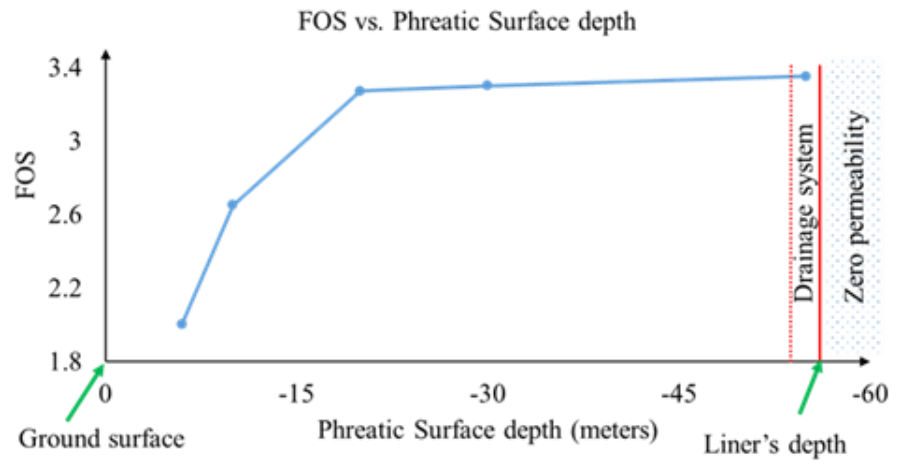


Fig. 4-9. The effect of phreatic surface depth on the FOS value.

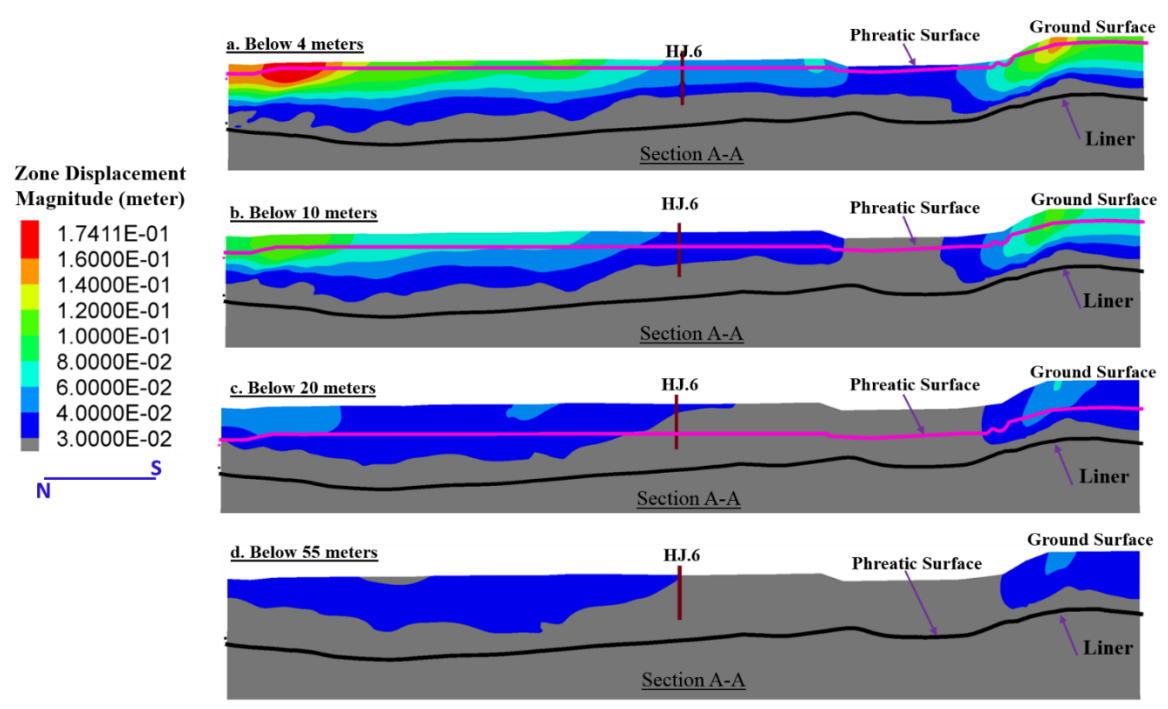


Fig. 4-10 The effect of phreatic surface depth on the displacement in the heap leach pad. The black line demarcates the liner location, and the purple line demarcates the phreatic surface.

The overburden pressure sets the lower limit of pressure to create rechanneling (increase the effective permeability) during the Hydro-Jex operation; ~5.0 bar is the minimum fluid pressure for 25 m depth at the location of HJ.6. This pressure creates non-zero effective stress during the operation and possibly a local weak sliding plane reinforced by the shear strength of the steel well casing with the solution pressure decreasing away from the well due to particle friction and drag. The worst case is considered to investigate the sliding instability; the pore pressure around the wells is set to the injection pressure ~5 bar (

Fig. 4-11) in an asynchronous manner (one zone and one well at a time).

A comparison between before and during the Hydro-Jex operation shows a decrease of FOS from 2.68 (before Hydro-Jex) to 2.65 (during Hydro-Jex). The 1.1% reduction suggests that the instability caused by the high-pressure injection is negligible. This refers to the fact that the area affected by the high-pressure injection (roughly a volume with 15 meters radius and 1.5 meters height) is much smaller than the heap dimensions. Also, the displacement contours remain nearly the same before (Fig. 4-7) and during (Fig. 4-12) the Hydro-Jex operation. The maximum displacement shows a ~20% increase (as expected to increase the permeability) within the injection zone; however, the displacement around the well is roughly the same.

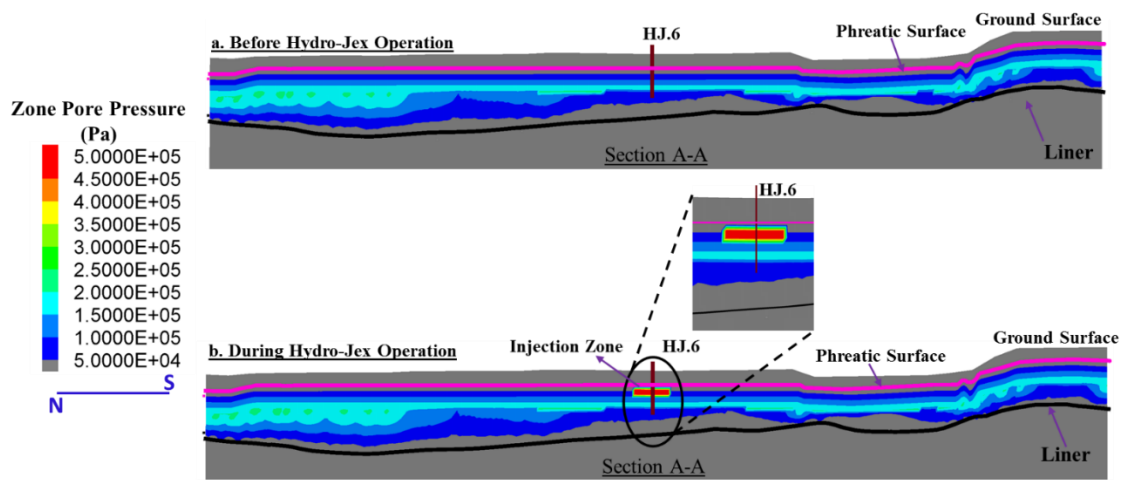


Fig. 4-11. Pore pressure counters before and during the Hydro-Jex operation. The black line demarcates the liner location, and the purple line demarcates the phreatic surface.

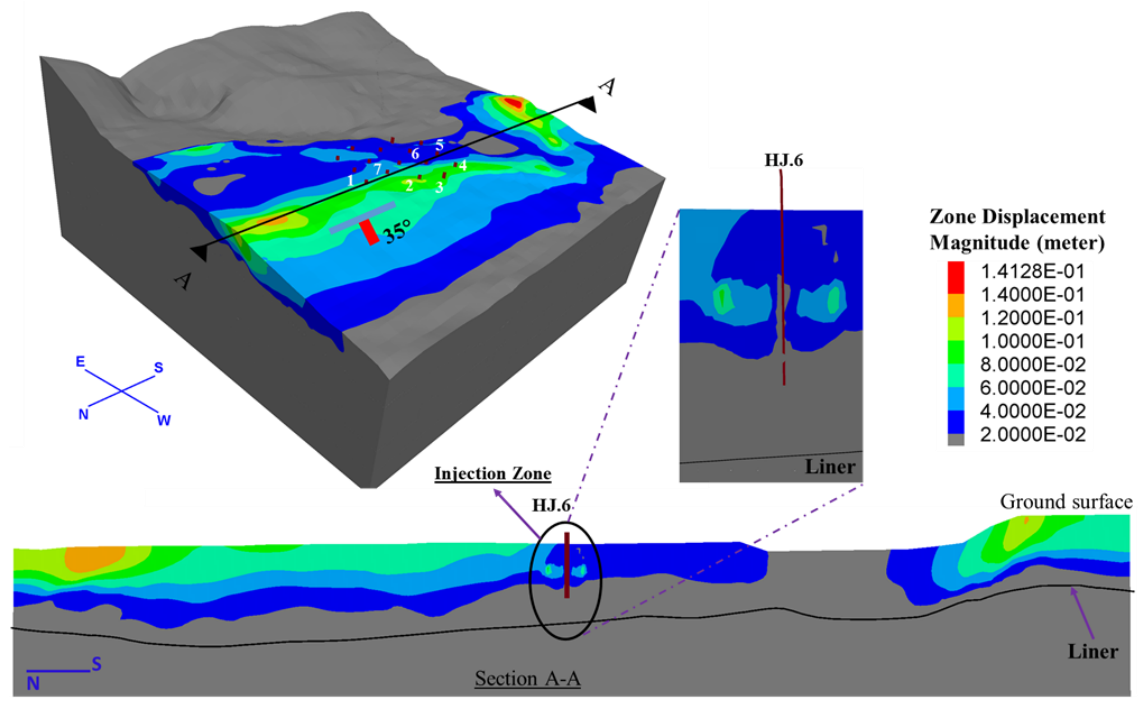


Fig. 4-12. Displacement of the heap leach pad during the Hydro-Jex operation wellbore HJ.6. The black line demarcates the liner location.

A sensitivity analysis shows that increasing the injection pressure more than 6.0 bar (at 25 m depth) causes instability in the heap leach pad (Fig. 4-13). The analysis indicates that the safety zone for the working pressure is between five to six bar and the heap can bear up to 25% above the overburden pressure. The results of displacement analysis (Fig. 4-14) shows that the high-pressure injection (up to 6.75 bar) do not affect the liner integrity, whereas mass and pressure need to increase significantly to exert a downward force on the liner.

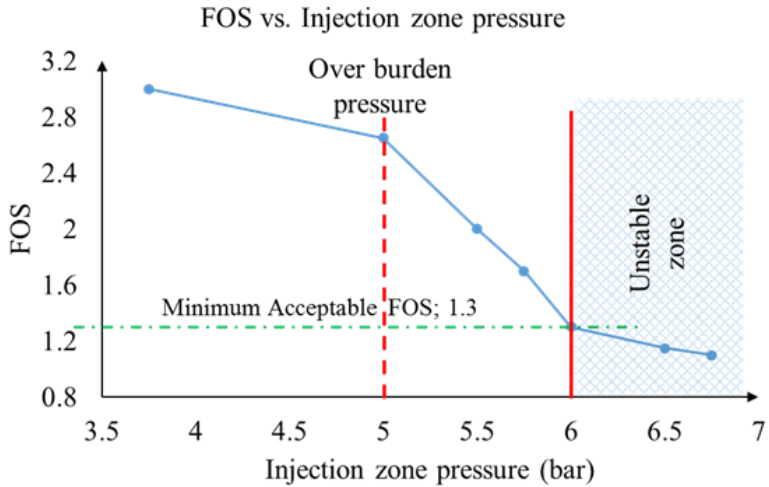


Fig. 4-13. The effect of injection zone pressure on FOS.

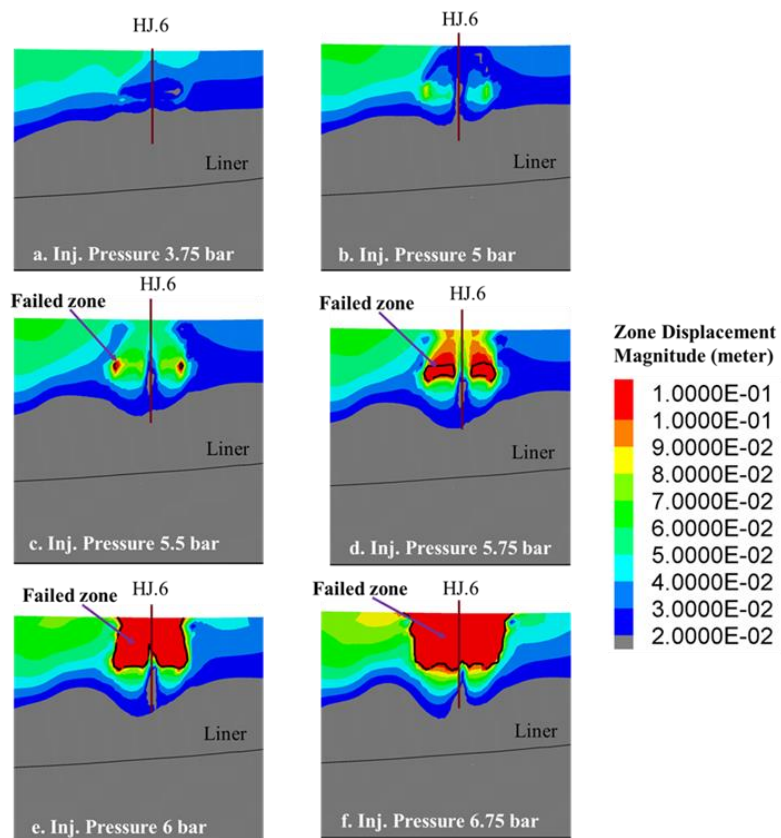


Fig. 4-14. The effect of injection zone pressure on the displacement around the well. The red area inside the black line shows the failed zone.

Acknowledgment:

The material of present chapter has been submitted for publishing in the “Mining, Metallurgy & Exploration” journal with the title of “The Effect of Hydro-Jex Operation on the Stability of Heap Leach Pads: A Case Study of the Los Filos Mine, Mexico.” The author would like to thank the co-authors of the paper Dr. Seyedsaeid Ahmadvand, Dr. Thom Seal, Dr. Bryan Ulrich and Dr. Behrooz Abbasi for their contribution.

5. Chapter 5 – Summary of the results and conclusion

5.1. Summary of Results

5.1.1. The Effect of Fault Zone on Rock Structure Stability

In this study, the slope stability of a single mine bench in the small and laboratory scales and of a whole open-pit mine in the large-scale were investigated in the presence of fault zones. Comparative and sensitive analyses were performed using three fault modeling methods and different initial conditions, and the effects were studied on the FOS of different models. Among the fault modeling methods, the ubiquitous joint (UJ) exhibited the highest sensitivity to the initial condition, and weak zone (WZ) exhibited the lowest. This trend was almost the same for the magnitude of the resulting FOS obtained by the latter two methods. Although the UJ method employs more considerations in the fault modeling, its high sensitivity suggests this method's better capability only when initial conditions are reliably collected.

Moreover, the UJ method is incapable of representing the direct shear and thus the correct behavior of continuous features. Especially in undulating nonplanar models, the UJ method cannot capture the failure in the fault zone and consequently overestimates the FOS. The mesh density analysis indicates that after a certain threshold, the higher resulting accuracy is negligible compared to the increase of the computational cost. The comprehensive comparison of three numerical methods of for fault material simulation is summarized in Table 5-1. This study infers that cohesion and friction angle should not have the same reduction factor in the SSR method, as their efficacy on the FOS suggests. The

large-scale modeling implies the initiation of failure from the bottom of the fault, propagation of shear stress along the fault, and tension stress towards the rock mass. A comparison between numerical and laboratory experiments indicates a better agreement between the two when the UJ and IF methods are used. However, more laboratory tests are under investigation to increase the level of sophistication and comparability between the theoretical and experimental stability tests on rock material.

Table 5-1 Comprehensive comparison of three numerical methods for fault material simulation

Method	Advantage	Disadvantage	Comments
Weak Zone (WZ)	<ul style="list-style-type: none"> • Easy to build complex geometry • Conservative method for estimating the FOS value. • Suitable method when working with low accurate data • Low sensitivity to mesh size • Low sensitivity to solve ratio 	<ul style="list-style-type: none"> • Possibility of the underestimate of FOS, especially in large scale and complex modeling • Cannot capture the orientation of discontinuities • Cannot capture the correct mechanism of failure (tend to show toppling behavior) • Requires at least three elements along fault thickness to capture the displacement • Shows the lowest consistency with the laboratory results. 	<ul style="list-style-type: none"> • The Lowest sensitivity concerning the input parameters, and fault geometry • This technique does not require high experience to build the model

Method	Advantage	Disadvantage	Comments
Ubiquitous-Joint (UJ)	<ul style="list-style-type: none"> • Considers the orientation of the planes of weakness (dip and dip direction) • Relatively easy to build complex geometry • Captures correct mechanics of failure • Good correlation with laboratory results 	<ul style="list-style-type: none"> • Possibility of overestimating of the FOS value • Sensitive to solve ratio, it requires low convergence value • Cannot consider the joint spacing, length, and stiffness • Cannot capture the correct behavior of continues feature • High sensitive to mesh size • Requires at least three elements along fault thickness to capture the displacement 	<ul style="list-style-type: none"> • Highest sensitivity concerning the input parameters, and fault geometry
Interface (IF)	<ul style="list-style-type: none"> • Can model the actual mechanical separation • Considers the orientation of the planes of weakness (dip and dip direction) • Captures correct mechanics of failure • Good correlation with laboratory results • Low sensitivity to mesh size • Low sensitivity to solve ratio 	<ul style="list-style-type: none"> • Cannot consider the fault zone thickness • Very difficult to build complex geological structures 	<ul style="list-style-type: none"> • Medium sensitivity concerning the input parameters, and fault geometry • This method requires a high level of expertise to build the complex geometry

5.1.2. The effect of Hydro-Jex technique on the stability of heap leach pad

In this research, monitoring the wells, phreatic surface, the permeability of the heap, fluid displacement, and the FOS were used prior after, and during the Hydro-Jex operation to analyze the stability of the heap leach pads at the Los Filos Mine. We demonstrate that the Hydro-Jex operation increases the permeability of the heap based on the saturation zone of the monitoring wells before and after the operation. As the permeability increases, the pore pressure and phreatic surface drop off, resulting in a grater slope for the heap. The FOS analysis suggests that the Hydro-Jex operation ideally improves the stability of the heap by 26%. The geophysical data attributes this significant improvement to the proper choice of drilling the Hydro-Jex wells, where over-compaction and physicochemical properties of the material results in water solution build-ups in the heap leach pads of the Los Filos Mine. In such cases, the high-pressure injection can break the over-compaction and release the water solution build-ups to drain down the HJ well post injection. Using the overburden and higher-pressure limits (<25%), numerical modeling dismisses any significant instability of the heap induced by the injection pressure. Therefore, it can be inferred that the instability stemming from the high-pressure injection is insignificant compared to the dimensionality of the heap during the Hydro-Jex operation. Also, displacement analysis indicates that the liner integrity remains intact at high injection pressure, even in the unstable zone.

5.2.Future Work

The proposed experimental method in this study to evaluate the numerical simulation result for finding FOS of the slope is applicable for non-cohesive fault materials. Extension

of the proposed method for large scale simulation (include several benches) and implementation of cohesive material for fault zone can be a good addition to this study. The focus of this study is limited to the fault zone effect on the stability of open-pit mine. A comprehensive study on the effect of other geological discontinuities like bedding plane is strongly recommended.

References

- Abbasi, B., Russell, D., & Taghavi, R. (2013). FLAC3D mesh and zone quality. In *FLAC/DEM Symposium*. China: Itasca Consulting Group.
- Alejano, L. R., & Alonso, E. (2005). Considerations of the dilatancy angle in rocks and rock masses. *International Journal of Rock Mechanics and Mining Sciences*, 42(4), 481–507. <https://doi.org/10.1016/j.ijrmms.2005.01.003>
- Alzo'ubi, A. K. (2016). Modeling yield propagation of jointed synthetic rock. In *Rock Mechanics and Rock Engineering: From the Past to the Future*. CRC Press, Tylor&Francis Group.
- Anon., (2018). <http://www.wise-uranium.org>. [Online], Available at: <http://www.wise-uranium.org/mdaf.html>
- Azarfar, B., Peik, B., Abbasi, B., & Roghanchi, P. (2018). A Discussion on Numerical Modeling of Fault for Large Open Pit Mines. 52nd US Rock Mechanics/Geomechanics Symposium, Seattle, Washington: American Rock Mechanics Association.
- Basi, J., Rucker, D. & Seal, T., (2017). Testing Inventory Drawdown through Pressure Injection in the Leach Pad at Los Filos Mine. Vancouver, BC, Canada, Conference of Metallurgists hosting World Gold & Nickel-Cobalt.
- Bishop, A. W. (1955). The use of the Slip Circle in the Stability Analysis of Slopes. *Géotechnique*, 5(1), 7–17. <https://doi.org/10.1680/geot.1955.5.1.7>

- Cala, M., Flisiak, J., & Tajdus, A. (2006). Slope stability analysis with FLAC in 2D and 3D. In 4th International FLAC Symposium on Numerical Modeling in the Geomechanics. Madrid.
- Chen, H., Chen, Y., Long, X. & Zou, Z., (2015). FLAC3D-based Improvement of the Strength Reduction Method's Slope Stability. *The Electronic Journal of Geotechnical Engineering*, Vol.20, Bund 24, pp. 12075-12088.
- Coulibaly, Y., Tikou, B. & Cheng, L., (2017). Numerical analysis and geophysical monitoring for stability assessment of the Northwest tailings dam at Westwood Mine. *International Journal of Mining Science and Technology*, Volume 27, pp. 701-710.
- Dawson, E. M., Roth, W. H., & Drescher, A. (1999). Slope stability analysis by strength reduction. *Géotechnique*, 49(6), 835–840. <https://doi.org/10.1680/geot.1999.49.6.835>
- Duncan, J. M. (1996). State of the Art: Limit Equilibrium and Finite-Element Analysis of Slopes. *Journal of Geotechnical Engineering*, 122(7), 577–596. [https://doi.org/10.1061/\(ASCE\)0733-9410\(1996\)122:7\(577\)](https://doi.org/10.1061/(ASCE)0733-9410(1996)122:7(577))
- Fleurisson, J.-A. (2012). Slope Design and Implementation in Open Pit Mines: Geological and Geomechanical Approach. *Procedia Engineering*, 46, 27–38. <https://doi.org/10.1016/j.proeng.2012.09.442>
- Franz, J. (2009). An investigation of combined failure mechanisms in large scale open pit slopes. University of New South Wales, Australia.
- Fu, X. et al., (2017). Computation of the safety factor for slope stability using discontinuous

deformation analysis and the vector sum method. *Computers and Geotechnics* 92, pp. 68-76.

Ghavidel, A., Mousavi, S. R., & Rashki, M. (2018). The Effect of FEM Mesh Density on the Failure Probability Analysis of Structures. *KSCE Journal of Civil Engineering*, 22(7), 2370–2383. <https://doi.org/10.1007/s12205-017-1437-5>

Ghorbani, Y., Franzidis, J. & Petersen, J., (2016). Heap Leaching Technology—Current State, Innovations, and Future Directions: A Review. *Mineral Processing and Extractive Metallurgy Review*, 37(2), pp.73-119., 37(2), pp. 73-119.

Gupta, V., Bhasin, R. K., Kaynia, A. M., Kumar, V., Saini, A. S., Tandon, R. S., & Pabst, T. (2016). Finite element analysis of failed slope by shear strength reduction technique: a case study for Surabhi Resort Landslide, Mussoorie township, Garhwal Himalaya. *Geomatics, Natural Hazards and Risk*, 7(5), 1677–1690. <https://doi.org/10.1080/19475705.2015.1102778>

Hammah, R. ., Yacoub, T., Corkum, B., Wibowo, F., & Curran, J. H. (2007). Analysis of Blocky Rock Slopes with Finite Element Shear Strength Reduction Analysis. In 1st Canada-U.S. Rock Mechanics Symposium (pp. 329–334). Vancouver, Canada:

Itasca. (2017). *FLAC3D (Fast Lagrangian Analysis of Continua in 3 Dimensions)*. Minneapolis: Itasca Consulting Group.

JIANG, Q. (2009). Strength reduction method for slope based on a ubiquitous-joint criterion and its application. *Mining Science and Technology (China)*, 19(4), 452–456. [https://doi.org/10.1016/S1674-5264\(09\)60084-3](https://doi.org/10.1016/S1674-5264(09)60084-3)

- Kalkani, E., (1976). The Rock Slope Stability Problem and the Application of 2-D F.E.A. to Rock Slope Stability and Comparison with Actual Failure. s.l., Purdue University.
- Karimi Nasab, S., Atashpanjeh, A. & Mollaei Fard, M., (2001). Design Considerations of Heap Leaching at Sarcheshmeh Open Pit Copper Mine. s.l., 17th International Mining Congress and Exhibition of Turkey- IMCET2001,.
- Khoei, A. R., (2015). Extended Finite Element Method: Theory and Applications. 1 edition ed. s.l.:Wiley.
- Kristiono, T. A. A., Pratama, D. Y., Pujiastuti, S. k. & Sophian, I., (2015). Pit Wall Failure Analysis on the West Wall of Batu Hijau Open Pit Mine, PT. Newmont Nusa Tenggara, Indonesia. Engineering Geology for Society and Territory, Volume 2, pp. 797-800.
- Kunkel, J., (2009). Geotech presentation on Hydro-Jex, Permitting, and Geotechnical Aspects. Knight Piesold.
- Lambert, C. & Coll, C., (2014). Discrete modeling of rock joints with a smooth-joint contact model. Journal of Rock Mechanics and Geotechnical Engineering, Issue 6, pp. 1-12.
- Mandziak, T. & Pattinson, D., (2015). Experience-based approach to successful heap leach pad design. Mining World, 12(5), pp. 28-35.
- Matsui, T., & San, K. . (1992). Finite element slope stability analysis by shear strength reduction technique. SOILS AND FOUNDATIONS, 32(1), 59–70.

<https://doi.org/10.3208/sandf1972.32.59>

Mortazavi, A. et al., (2015). Geotechnical investigation and design of leaching heap No. 2, Meydook copper mine, Iran. *Minerals Engineering*, Volume 79, pp. 185-195.

Mostyn, G., Helgstedt, M. D., & Douglas, K. J. (1997). Towards field bounds on rock mass failure criteria. *International Journal of Rock Mechanics and Mining Sciences*, 34(3–4), 208.e1-208.e18. [https://doi.org/10.1016/S1365-1609\(97\)00163-9](https://doi.org/10.1016/S1365-1609(97)00163-9)

Padilla, G. A., Cisternas, L. A. & Cuetoa, J. Y., (2008). On the Optimization of Heap Leaching;. *Minerals Engineering*, 21(9), pp. 673-678.

Park, D., & Michalowski, R. L. (2017). Three-dimensional stability analysis of slopes in hard soil/soft rock with tensile strength cut-off. *Engineering Geology*, 229, 73–84. <https://doi.org/10.1016/j.enggeo.2017.09.018>

Paterson, M. S., (1978). *Experimental Rock Deformation – the Brittle Field*. Berlin: Springer.

Patton, F. D., (1966). Multiple modes of shear failure in rock. Lisbon, 1st. Congr, Int. Soc. Rock Mech, pp. 509-513.

Petersen, J., (2016). Heap leaching as a key technology for recovery of values from low-grade ores – A brief overview. *Hydrometallurgy*, Volume 165, pp. 206-212.

Plumlee, G. S., Edelman, P. & Bigelow, R. C., (1995). *The Summitville Mine and Its Downstream Effects*, s.l.: USGS.

Price, D. G., (2009). *Engineering Geology, Principles and Practice*. s.l.:Springer.

- Raghuvanshi, T. K. (2019). Plane failure in rock slopes – A review on stability analysis techniques. *Journal of King Saud University - Science*, 31(1), 101–109. <https://doi.org/10.1016/j.jksus.2017.06.004>
- Reddy, D., Balderrama, R., Sterling, P. & Arseneau, G., (2018). Technical Report for Los Filos Gold Mine, Vancouver, B.C.: Leagold Mining Corporation.
- Reyes, A. et al., (2016). 3D dynamic analysis of a valley-fill heap leach pad. Lima, Peru, InfoMine, © 2016 InfoMine, ISBN: 978-1-988185-03-3.
- Reyes, A., Garma, P. & Parra, D., (2014). 3D slope stability analysis of heap leach pads using the limit equilibrium method. Lima, Peru, InfoMine, © 2014 InfoMine, ISBN: 978-0-9917905-6-2.
- Rose, N. D. & Hungr, O., (2007). Forecasting potential rock slope failure in open pit mines using the inverse-velocity method. *International Journal of Rock Mechanics and Mining Sciences*, 44(2), pp. 308-320.
- Rucker, D. F., (2015). Deep well rinsing of a copper oxide heap. *Hydrometallurgy*, Volume 153, pp. 145-153.
- Rucker, D. F., McNeill, M., Schindler, A. & Noonan, G., (2009). Monitoring of a Secondary Recovery Application of Leachate Injection into a Heap. *Hydrometallurgy*, Volume 99, pp. 238-248.
- Sainsbury, B. L., & Sainsbury, D. P. (2017). Practical Use of the Ubiquitous-Joint Constitutive Model for the Simulation of Anisotropic Rock Masses. *Rock Mechanics*

and Rock Engineering, 50(6), 1507–1528. <https://doi.org/10.1007/s00603-017-1177-3>

Seal, T., (2004). Enhanced Gold Extraction in Cyanide Heap Leaching Using Hydro-Jex, s.l.: Ph.D. Dissertation, University of Idaho..

Seal, T., (2007). HYDRO-JEX: Heap Leach Pad Stimulation Technology' Ready for World Wide Industrial Adoption?. Denver Colorado, USA, SME.

Seal, T. & Jung, S., (2005). Reduction of Gold Inventory in Cyanide Heap Leaching.. s.l., SME Annual Meeting: Got Mining — Preprints, pp. 163–167.

Seal, T., Rucker, D., Winterton, J. & Ashanti, A., (2012). Enhancing Gold Recovery using Hydro-Jex© at Cripple Creek and Victor Gold Mine Co.. Denver, SME.

Septian, A., Llano-Serna, M., Ruest, M. & Williams, D., (2017). Three-dimensional Kinematic Analysis of Bingham Canyon Mine Pit Wall Slides. s.l., s.n., pp. 86-93.

Sharma, R. ., & Kaur, A. (2016). Slope stability analysis techniques: a review. International Journal of Engineering Applied Sciences and Technology, 1(4), 52–57.

Sjoberg, J., Hustrulid, W. A., McCarter, M. K., & Van Zyl, D. J. A. (2000). Failure Mechanisms for High Slopes in Hard Rock. In International conference; 4th, Stability in open pit mining (pp. 71–80). Littleton, CO: Society for Mining, Metallurgy, and Exploration.

Stacey, T., Xianbin, Y., Armstrong, R., & Keyter, G. (2003). New slope stability considerations for deep open pit mines. The Journal of The South African Institute of

Mining and Metallurgy, 103, 373–390.

Stead, D., & Wolter, A. (2015). A critical review of rock slope failure mechanisms: The importance of structural geology. *Journal of Structural Geology*, 74, 1–23. <https://doi.org/10.1016/j.jsg.2015.02.002>

Sun, C., Chai, J., Xu, Z., Qin, Y., & Chen, X. (2016). Stability charts for rock mass slopes based on the Hoek-Brown strength reduction technique. *Engineering Geology*, 214, 94–106. <https://doi.org/10.1016/j.enggeo.2016.09.017>

Taleb Hosni, A., & Berga, A. (2016). Assessment of Slope Stability by Continuum and Discontinuum Methods. In 18th International Conference on Civil and Geological Engineering. Istanbul, Turkey.

Tang, S. B., Huang, R. Q., Tang, C. A., Liang, Z. Z., & Heap, M. J. (2017). The failure processes analysis of rock slope using numerical modelling techniques. *Engineering Failure Analysis*, 79, 999–1016. <https://doi.org/10.1016/j.engfailanal.2017.06.029>

Tutluoglu, L., Ferid Öge, I., & Karpuz, C. (2011). Two and three dimensional analysis of a slope failure in a lignite mine. *Computers & Geosciences*, 37(2), 232–240. <https://doi.org/10.1016/j.cageo.2010.09.004>

Ulrich, B., (2008). Geotechnical Aspects of the Hydro-Jex Operation. Perth, Australia, s.n.

Vermeer, P. A. (1998). Non-Associated Plasticity for Soils, Concrete and Rock. In *Physics of Dry Granular Media* (pp. 163–196). Dordrecht: Springer Netherlands. https://doi.org/10.1007/978-94-017-2653-5_10

- Yang, P., Zhu, Z. Y., & Zou, Z. Y. (2012). Study on Strength Reduction Method with Two Reduction-Factors. *Applied Mechanics and Materials*, 204–208, 429–433. <https://doi.org/10.4028/www.scientific.net/AMM.204-208.429>
- You, G., Mandalawi, M. Al, Soliman, A., Dowling, K., & Dahlhaus, P. (2018). Finite Element Analysis of Rock Slope Stability Using Shear Strength Reduction Method (pp. 227–235). https://doi.org/10.1007/978-3-319-61902-6_18
- Wiles, T., (2014). Three ways to assess mining-induced fault instability using numerical modelling. s.l., s.n.
- Winterton, J. & Rucker, D., (2013). Optimal Strategies for Leach Pad Injection Operations. Phoenix, AZ. Society of Mining Metallurgical and Exploration (SME) Annual Meeting
- Zanbak, C., (2012). HEAP LEACHING TECHNIQUE in MINING Within the Context of BEST AVAILABLE TECHNIQUES, s.l.: Euromines, The European Association of Mining Industries, Metal Ores & Industrial Minerals.
- Zhang, K., Cao, P., Liu, Z., Hu, H., & Gong, D. (2011). Simulation analysis on three-dimensional slope failure under different conditions. *Transactions of Nonferrous Metals Society of China*, 21(11), 2490–2502. [https://doi.org/10.1016/S1003-6326\(11\)61041-8](https://doi.org/10.1016/S1003-6326(11)61041-8)
- Zheng, Y., Chen, C. X., Zhu, X. X., Liu, X. M., & Cheng, G. W. (2013). Stability Analysis of Open-Pit Slope Containing a Fault Utilizing UDEC. *Applied Mechanics and Materials*, 444–445, 1204–1210.

<https://doi.org/10.4028/www.scientific.net/AMM.444-445.1204>

Zienkiewicz, O. C., Humpheson, C., & Lewis, R. W. (1975). Associated and non-associated visco-plasticity and plasticity in soil mechanics. *Géotechnique*, 25(4), 671–689. <https://doi.org/10.1680/geot.1975.25.4.671>